Negative-U extended Hubbard model for doped barium bismuthates

A. Taraphder*
NEC Research Institute, Inc., 4 Independence Way, Princeton, New Jersey 08540;
Serin Physics Laboratory, Rutgers University, Piscataway, New Jersey 08855;
and Department of Physics, Indian Institute of Science, Bangalore 560012, India

H. R. Krishnamurthy,* Rahul Pandit,* and T. V. Ramakrishnan†
Department of Physics, Indian Institute of Science, Bangalore 560012, India

We present detailed mean-field and random-phase-approximation studies of the negative-U, extended Hubbard model with a view to understanding the properties of the doped barium bismuthates. In particular, we obtain the phase diagram, the excitation spectrum, and the optical conductivity in the semiconducting phase of the bismuthates. We show by explicit calculations how this model leads to a natural explanation for the two, well-separated transport and optical gaps observed in the semiconducting phases of the bismuthates. We fix the parameters in our model by fitting these experimentally observed gaps; and with these parameter values we compute other properties of these systems. We also show how metallic screening and disorder can decrease the superconducting T_c dramatically. Our theory leads to an exotic charge-transport mechanism, dominated by charge $\pm 2e$ bosons (cooperons), in the semiconducting phases of these systems.

I. INTRODUCTION

The materials $BaPb_{1-x}Bi_xO_3$ and $Ba_{1-x}K_xBiO_3$ have drawn a lot of attention over the past few years. This interest stems principally from their superconducting T_c's (13 and 34 K for Pb and K doping, respectively) which are 3–5 times higher than for other three-dimensional oxides with similar, *low* densities of states at the Fermi level.[1,2] In addition these materials exhibit charge-density-wave (semiconducting) and metallic phases; transitions from one phase to the other occur as the doping or temperature are changed.[1,2]

A negative-U, extended Hubbard model was proposed for these systems by Rice and co-workers,[3] who suggested that the negative U arises because of electron-phonon interactions. However, Varma[4] has recently proposed that the negative U occurs because of electronic processes in the solid, coupled with the chemistry of valence skipping displayed by the bismuth ion (see below). In a recent article[5] (henceforth referred to as I) we have studied some of the consequences of the negative-U, extended Hubbard model for these bismuthates, focusing on what we believe is one of the *key issues* here: whether the source of the negative U and the superconductivity is *phonon mediated* or *electronic*. We have shown that, if the negative U has an electronic origin, then the semiconducting charge-density-wave (CDW) phase of these materials is *unique*, in that charge $\pm 2e$ bosonic bound states (cooperons) of two electrons or two holes dominate its transport properties. We have also shown that this offers a natural explanation for the remarkable difference between the optical and the transport gaps observed in these systems.

We have argued elsewhere[2] that the large-U limit of the negative-U extended Hubbard model, studied by many authors,[4] is inadequate for a realistic description of these bismuthates (at the simplest level because the superconducting coherence length is too small compared to those found experimentally). In I we showed that the intermediate-U regime of this model is far more suitable for this purpose; and we summarized our theoretical findings for this regime. (We display the negative sign of U explicitly when required and take U itself to be positive.) In this paper we give the details of the calculations that led to our results in I. Furthermore, we evaluate critically the feasibility of using the negative-U, extended Hubbard model for these bismuthates by fitting a variety of experimentally measured quantities, such as the optical and transport-activation gaps in the semiconducting phase, the superconducting transition temperature and the superconducting coherence length. In the remaining part of this introduction we give a brief summary of the experimental findings that have led us and other workers to use the negative-U, extended Hubbard model for these bismuthates, a brief list of our principal results, and a plan of this paper.

A. Summary of experimental results

Systems like $BaPb_{1-x}Bi_xO_3$ (Ref. 6) and $Ba_{1-x}K_xBiO_3$ (Ref. 7) are intriguing as they show remarkably high superconducting transition temperatures[1,7] in spite of being three dimensional and having small densities of states at their Fermi levels. Other important experimental findings are

(1) Their structures are slight distortions of a cubic perovskite.[1,6,8,9] Bi (or Pb) atoms occupy the cube corners, O atoms the face centers, and Ba (or K) atoms the body centers; each Bi atom lies at the center of an octahedron of O atoms. Slight distortions or rotations of these octahedra lead to many structural transitions.[1,6–12]

In pure $BaBiO_3$ the octahedra are alternately dilated and contracted: there are two distinct nearest-neighbor Bi-O distances differing by $\simeq 10\%$. Powder-neutron-diffraction measurements on $Ba_{1-x}K_xBiO_3$ show a frozen, breathing-mode distortion of the oxygen octahedra in the monoclinic phase, but not in any of the other semiconducting phases.[10,13] In the semiconducting region (at least for the lead-doped system) the bismuth ion has a tendency to skip the valence 4^+, its formal valence in both the potassium- and lead-doped systems, and forms a three-dimensional, charge-disproportionated structure[9,13] with alternating "3^+" and "5^+"ions.

(2) $BaBiO_3$ doped with Pb or K exhibits semiconducting, metallic, and superconducting phases.

(3) $BaBiO_3$ is a diamagnetic (not a Mott) insulator,[6,9] even though it has a half-filled Bi6*s*-O2*p* band.[14] Both the potassium- and lead-doped systems are diamagnetic in the entire ranges of concentrations studied so far. The diamagnetic susceptibility is essentially a very small paramagnetic contribution from the valence electrons added to the large diamagnetic contributions from the atomic cores.

(4) The semiconducting phases of these bismuthates persist for an unusually large range of doping with Pb ($0.35 < x < 1$) which changes both the local correlation and the electron concentration, and K doping ($x < 0.6$) which changes only the latter. In both cases, there is considerable disorder. The properties of the semiconducting phase are unconventional. For example, in $BaPb_{1-x}Bi_xO_3$ transport-activation and optical gaps[2,6,15] differ by nearly an order of magnitude (for $x = 1$ the transport and optical gaps are, respectively, 0.24 and 2 eV). The temperature dependence of the resistivity shows that the transport-activation gap increases from 0 at $x = 0.35$ to 0.24 eV at $x = 1$. This transport gap does not show up in photoconductivity, optical-absorption, or photoacoustic measurements. At $x = 1$ the carrier concentration $n(T) = 1.1 \times 10^{22}(\mathrm{cm}^{-3})\exp(-0.24\ \mathrm{eV}/k_B T)$; the large pre-exponential factor[2,6] indicates an intrinsic transport mechanism. In optical-conductivity spectra, the metal-semiconductor transition is marked by a transfer of the spectral weight into a high-frequency peak that grows, with increasing x, into a peak containing nearly all the spectral weight.[6,15]

(5) $BaPb_{1-x}Bi_xO_3$ has a fairly high resistivity (540 $\mu\Omega$ cm at $x = 0.24$) throughout its metallic range ($0 < x < 0.35$); this resistivity is nearly temperature independent. Carrier concentrations in the metallic phases of these bismuthates are surprisingly small ($\simeq 10^{21}\ \mathrm{cm}^{-3}$) and transport properties have an anomalous temperature dependence for $0.2 < x < 0.35$. In the same region of x values, the ac conductivity deviates from the Drude form. We note that this is well before the metal-semiconductor transition, which occurs for $x \simeq 0.35$. The dependence of the specific heat on the temperature T shows slight deviations from linearity at low T.[16] Resistivity measurements[17] on thin films of $Ba_{1-x}K_xBiO_3$ show a linear dependence on T from T_c up to room temperature though the extrapolated residual resistivity is rather high $\simeq 250$ $\mu\Omega$ cm. Tunneling measurements show[18,19] a linear, V-shaped tunneling density of states somewhat similar to those in cuprate superconductors.

(6) For the potassium-doped (lead-doped) system the maximum T_c for superconductivity is 34 K (13 K).[6,9] The observed densities of states at the Fermi levels for both these systems are very low compared to conventional superconductors. In addition, a variety of experiments yield $2\Delta/k_B T_c$ close to the BCS value of 3.5,[18,19] a considerable isotope effect,[9,11] and a superconducting coherence length around 70-80 A.

B. Theoretical conclusions

Since some of the basic features of these barium bismuthates suggest an effective local attraction between electrons, we explore the properties of such a model, and compare our results with the unusual behavior summarized above. We study a tight-binding model for electrons on a cubic lattice, with negative (attractive) on-site U, and a nearest-neighbor repulsion V (i.e., an extended, negative-U Hubbard model). The V term is indicated since it stabilizes a charge-disproportionated state, which (for $V = 0$) is degenerate with a superconducting, Cooper-pair state at half filling. We have analyzed this model (in the absence of any disorder) in a mean-field approximation, for the phase diagram, and in the random-phase/ladder approximations for various propagators and physical response functions. Our principal results are summarized below and calculational details given in subsequent sections.

(1) We obtain the mean-field phase diagram [Figs. 1(a) and 1(b)] of this model. We can distinguish between semiconducting (CDW), superconducting (*s*-wave and extended-*s*-wave), intermediate (both superconducting and CDW), and metallic phases. We find[5] that the intermediate phase is unstable with respect to phase separation into CDW and superconducting states in contrast to earlier claims.[20,21] Phase diagrams that are qualitatively similar to ours[2,5] have been obtained recently by Aharony and Auerbach[22] in the large-U limit where the model reduces to a spin model[21] whose mean-field phase diagram was studied in detail by Liu and Fisher.[23] Our phase diagram is in qualitative accord with experiments in so far as it exhibits three stable phases: a semiconductor (CDW), a singlet superconductor, and a nonordered metal. Phase transitions between all excepting CDW and superconducting phases are continuous; the superconductor-CDW transition is first order.

(2) If the negative value of U is electronic in origin [see point (7) below], then, in the CDW phase, there are two-particle and two-hole bound states, i.e., cooperons, with energies in the gap of the two-particle spectrum (Fig. 2). We calculate the pairing susceptibility in the ladder approximation in the particle-particle channel and use it to obtain these bound-state (cooperon) energies in the CDW phase. (In the large-U limit, this energy evolves smoothly into the anisotropy gap of the pseudospin-wave spectrum of the pseudospin model that obtains in this limit.[2]) The bound-state energy moves continuously towards the chemical potential as V, the nearest-neighbor Coulomb repulsion, approaches zero.

(3) These cooperons dominate charge transport in the

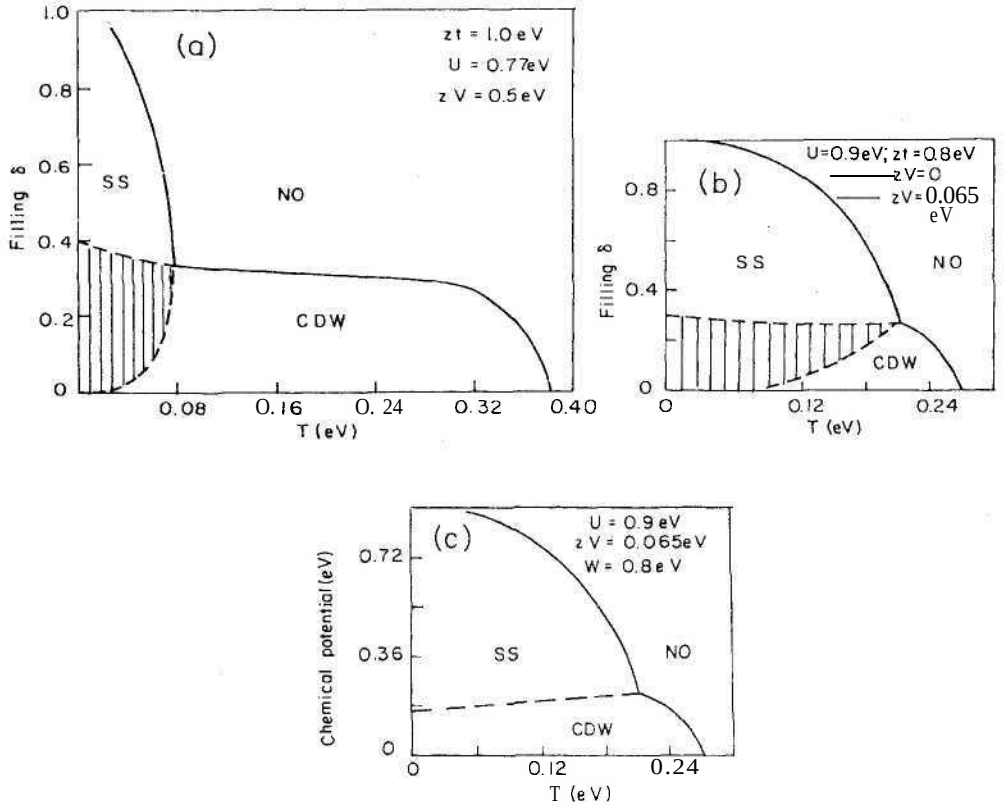

FIG. 1 (a) and (b) The mean-field phase diagrams of the negative-U, extended Hubbard model in the filling-temperature plane, for two different values of the interaction parameters. The solid lines are second-order phase boundaries that separate the nonordered metallic phase from the singlet superconducting (SS) and the charge-density-wave (CDW) phase. The hatched region is the two-phase coexistence region (SS and CDW) corresponding to the first-order phase boundary between CDW and SS phases (c). The values of Coulomb interactions and zt needed to obtain these phase diagrams are shown. (c) The mean-field phase diagram of the negative-U, extended Hubbard model in the chemical potential-temperature plane, with the same parameter values as in (b). The solid and the dashed lines denote continuous and first-order transitions, respectively.

CDW semiconducting phase. This possibility was qualitatively recognized in the bipolaron language by Uchida, Kitazawa, and Tanaka.[6] In the large-U limit this yields the conductivity mechanism that we have discussed elsewhere.[2,5] The random-phase-approximation (RPA) conductivity shows activated behavior with the activation energy equal to the particle-particle bound-state energy. In the CDW semiconducting phase, therefore, the transport gap is clearly different from the optical gap, which is the gap in the single-particle spectrum (twice the CDW gap parameter in the small-U regime, and $\simeq U$, for large U).

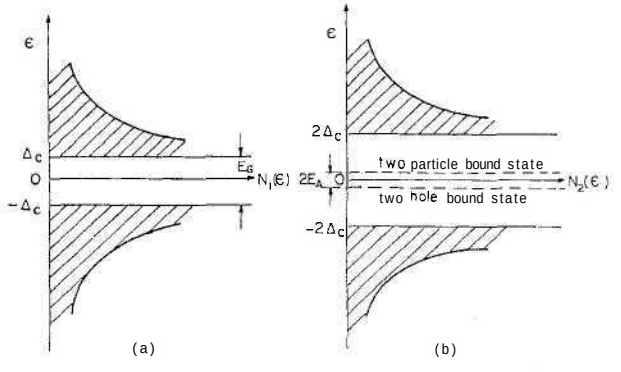

FIG. 2. (a) The single-particle excitation spectrum in the mean-field CDW phase where Δ_c is the CDW gap parameter. In (b) are shown the two-particle (hole) bound states that form inside the gap of the two-particle spectrum. The energy of these bound states (with respect to the chemical potential indicated as zero) is the transport gap (E_A) in our theory.

(4) Our RPA calculation of the optical conductivity in the single- and two-particle channels shows that, in the large-U limit, the conductivities in these two channels differ by nearly a factor of 10. This, together with possible nonperturbative orthogonality effects, may be the reason why the transport gap does not appear in optical measurements.

(5) At large U the pairs are tightly bound in real space and can be thought of as a quantum lattice gas of hard-core bosons (i.e., no more than one boson per site); at small U, k-space pairing is the proper description for these pairs. Our calculation yields a natural interpolation between these two limits at $T=0$.

(6) The ac conductivity in the metallic phase is of the Drude form. At large U the carriers are charge-$2e$, hard-core, bosons as we have discussed earlier;[2,5] at small U the metal is, of course, a conventional Fermi liquid. There is a smooth crossover between them which we do not investigate here.

(7) For the above explanation of the two gaps to be valid, the attractive, on-site interaction must be electronic in origin since an attraction mediated by phonons is retarded and operates only over some characteristic phonon frequency. Such an interaction cannot produce the necessary binding to form a two-particle bound state with binding energy $\simeq 1-2$ eV.

The remaining part of this paper is organized as fol-

lows: In Sec. II we describe our calculations in the intermediate-U regime of the negative-U, extended Hubbard model. We first describe our mean-field theory and the phase diagram we obtain from it. We then present our calculations for the excitation spectrum in the particle-particle channel, the pseudospin-wave spectrum in the large-U limit and the conductivity (corresponding to the mechanism of charge conduction in the CDW phase mentioned above). In Sec. III we conclude with a discussion of the strengths and weaknesses of this model, suggest future directions of study, and propose some experiments which can be used to verify our theory.

II. PHASE DIAGRAMS, ELEMENTARY EXCITATIONS AND RESPONSE FUNCTIONS

In Sec. II A we discuss our mean-field theory for the negative-U, extended Hubbard model. In Sec. II B we develop the formalism for calculating the two-particle excitation spectrum (i.e., the susceptibility in the Cooper channel).

A. Mean-field phase diagram

The one-band, negative-U, extended Hubbard Hamiltonian that we use (on a simple-cubic bismuth lattice) is

$$H=-t\sum_{\langle ij\rangle\sigma}c_{i\sigma}^{\dagger}c_{j\sigma}-\frac{U}{2}\sum_{i\sigma}\hat{n}_{i\sigma}\hat{n}_{i-\sigma}+\frac{V}{2}\sum_{\langle ij\rangle\sigma\sigma'}\hat{n}_{i\sigma}\hat{n}_{j\sigma'}\hat{r}_{j\sigma'}-\mu\sum_{ia}\hat{n}_{i\sigma}\ , \tag{1}$$

where t is the hopping matrix element between nearest-neighbor pairs of sites $\langle i,j\rangle$, U is the onsite attraction (see above), V is the nearest-neighbor Coulomb repulsion, and μ is the chemical potential. Reductions of a three-band model that includes Bi and O sites to such a one-band model have been discussed elsewhere.[2,4]

Though the qualitative features of the phase diagram of model (1) are known,[20] some earlier[20,21] mean-field treatments of it are not entirely correct.[24] We correct and extend the mean-field theory for model (1). The order parameters we use are

$$\langle c_{i\uparrow}^{\dagger}c_{i\downarrow}^{\dagger}\rangle=b_s^{*}\ ,$$
$$\langle c_{i\uparrow}^{\dagger}c_{j\downarrow}^{\dagger}\rangle=b_e^{*}\ ,$$
$$\langle c_{i\sigma}^{\dagger}c_{j\sigma}\rangle=C_0$$

and

$$\langle\hat{n}_{i\sigma}\rangle=\frac{n}{2}+\frac{b_c}{2}e^{i\mathbf{Q}\cdot\mathbf{r}_i}\ , \tag{2}$$

where $\mathbf{Q}=\pi/a(1,1,1)$, b_c is the CDW order parameter, b_s and b_e are, respectively, on-site and extended singlet-superconducting order parameters, and C_0 a self-consistent contribution to the bandwidth. Clearly our mean-field theory can distinguish between phases characterized by any one or a combination (as in the intermediate phase mentioned above) of these types of ordering. We consider only translationally invariant, real order parameters. A Hartree-Fock decoupling yields the mean-field Hamiltonian

$$H_{\mathrm{mf}}=-\sum_{\mathbf{k}\sigma}(\tilde{\epsilon}_{\mathbf{k}}+\bar{\mu})c_{\mathbf{k}\sigma}^{\dagger}c_{\mathbf{k}\sigma}-\Delta_c\sum_{\mathbf{k}\sigma}c_{\mathbf{k}+Q\sigma}^{\dagger}c_{\mathbf{k}\sigma}-\sum_{\mathbf{k}}\Delta_s(\mathbf{k})(c_{-\mathbf{k}\downarrow}c_{\mathbf{k}\uparrow}+c_{\mathbf{k}\uparrow}^{\dagger}c_{-\mathbf{k}\downarrow}^{\dagger})+N\left[Ub_s^2-Vzb_e^2+\frac{1}{4}n^2u_m+\frac{1}{4}b_c^2u_p+VzC_0^2\right]\ , \tag{3}$$

where N is the total number of lattice sites, $c_{\mathbf{k}\sigma}$ is the Fourier transform of $c_{i\sigma}$, and $u_m=U-2zV$, $u_p\equiv U+2zV$, $\bar{\mu}\equiv\mu+u_mn$, $\tilde{\epsilon}_{\mathbf{k}}=z\tilde{t}\gamma_{\mathbf{k}}$, $\tilde{t}=t+VC_0$, with $\gamma_{\mathbf{k}}=z^{-1}\sum_{\mathbf{a}}\exp(i\mathbf{k}\cdot\mathbf{a})$, $\{\mathbf{a}\}$ being the nearest-neighbor lattice vectors. The quantities $\Delta_c\equiv u_pb_c/2$ and $\Delta_s(\mathbf{k})\equiv Ub_s-zVb_e\gamma_{\mathbf{k}}$ are, respectively, the gap parameters in the CDW and superconducting phases.

The mean-field Hamiltonian (3) can be easily diagonalized (Appendix A) and the four eigenvalues we obtain are $\pm E_{\mathbf{k}}^{\pm}$, where $E_{\mathbf{k}}^{\pm}=[R_{\mathbf{k}}\pm2P_{\mathbf{k}}]^{1/2}$, $R_{\mathbf{k}}=\Delta_c^2+U^2b_s^2+V^2z^2b_e^2\gamma_{\mathbf{k}}^2+\bar{\mu}^2+\tilde{\epsilon}_{\mathbf{k}}^2$, and

$$P_{\mathbf{k}}=[(Ub_sVz\gamma_{\mathbf{k}}b_e+\bar{\mu}\tilde{\epsilon}_{\mathbf{k}})^2+\Delta_c^2(u^2b_s^2+\bar{\mu}^2)]^{1/2}\ ,$$

whence the mean-field free energy per site is (Appendix A):

$$f=-\frac{1}{N\beta}{\sum_{\mathbf{k}}}'\left[\ln\left\{4\cosh^2\left(\frac{\beta E_{\mathbf{k}}^{+}}{2}\right)\right\}+\ln\left\{4\cosh^2\left(\frac{\beta E_{\mathbf{k}}^{-}}{2}\right)\right\}\right]+Ub_s^2-Vzb_e^2+\frac{1}{4}n^2u_m+\frac{\Delta_c^2}{u_p}+zVC_0^2+\bar{\mu}(n-1)\ ,$$

where the prime over the summation sign indicates that k is restricted to half the Brillouin zone.

The self-consistency equations for the order parameters follow from a minimization of this free energy (Appendix B). We solve the self-consistency equations by a numerical, iteration method for different values of U/zt and V/zt (z, the number of nearest-neighbor sites, is six here) and the filling $\delta=n-1$. To find the stable phases we start from a large number of different initial values for the order parameters and ensure convergence by checking that successive iterates of the order parameters do not differ by more than 10^{-5}. If more than one solution is obtained, we choose the one which yields the lowest value of the free energy.

We show phase diagrams in both filling-temperature [Figs. 1(a) and 1(b)] and chemical potential-temperature [Fig. 1(c)] planes. The topology of the phase diagram is the same as in the large-U case[2] but the positions of phase boundaries, etc., are quite different. There are three thermodynamically stable phases: A CDW phase ($C_0\neq0$, $\Delta_c\neq0$ and $b_s=b_e=0$); separated from this CDW phase by a first-order line in the μ-T plane is the superconducting phase ($C_0\neq0$, $b_s\neq0$, $b_e\neq0$ and $\Delta_c=0$); and the nonordered, metallic phase (all the order parameters except C_0 are zero) at high temperature (at S = 1 this phase goes down to $T=0$). The phase transitions between the

ordered phases and the nonordered phase are all continuous. The two lines of continuous transitions meet at a bicritical point. The first-order line in the T-μ phase diagram [Fig. 1(c)] opens out into a region of two-phase coexistence (CDW and superconducting phases) in the T-δ phase diagram [Figs. Ha) and 1(b)].

For $V=0$ and $\delta=0$ in model (1) the CDW and superconductor solutions of the self-consistency equations are connected by a pseudospin-rotation symmetry[25,26] of the Hamiltonian and hence are degenerate; their free energies are equal and they coexist. Away from half filling this degeneracy is removed and the superconducting phase becomes stable. The degeneracy between CDW and superconducting phases is also lifted when V becomes nonzero: at half filling the CDW phase is the thermodynamically stable one; of course, sufficiently far away from half filling, the superconducting phase becomes stable.

Typical phase diagrams are shown in Figs. l(a)-l(c). For comparison, we give the filling-temperature phase diagram for two different sets of values of U/zt and V/zt. Full lines indicate continuous, second-order phase boundaries and the dashed line in Fig. l(c) indicates a first-order boundary. The hatched regions in Figs. 1(a) and Kb) are the two-phase coexistence regions. In these two-phase region (and in equilibrium) the system phase separates into semiconducting (CDW) and superconducting phases, with one interface between them.

The equations for the two boundaries separating the ordered phases from the disordered phase can be obtained explicitly (Appendix C). The gap equation for the CDW gap parameter is

$$\frac{1}{u_p}=\frac{1}{2}\int_{-W}^{+W}\rho(\epsilon)\frac{\tanh[(1/2)\beta(\epsilon^2+\Delta_c^2)^{1/2}-\bar{\mu}]}{(\epsilon^2+\Delta_c^2)^{1/2}}d\epsilon\ , \quad (4)$$

where $2W$ is the noninteracting bandwidth. At half filling $\bar{\mu}=0$ and if we take the density of states $\rho(\epsilon)$ to be a constant, then this gap equation assumes the BCS form

$$\frac{1}{u_p}=\frac{1}{4W}\int_{-W}^{+W}\frac{\tanh(1/2)\beta(\epsilon^2+\Delta_c^2)^{1/2}}{(\epsilon^2+\Delta_c^2)^{1/2}}\text{-}de\ ,$$

from which the CDW-nonordered (metal) transition temperature T_{CD} is obtained by setting $\Delta_c=0$ at this temperature. Thus we get (the BCS form) $T_{\mathrm{CD}}=2\gamma/\pi We^{-2W/\beta}$, where γ is the Euler constant and $2\gamma/\pi\simeq 1.13$. At $T\equiv 1/\beta=0$ straightforward integration yields the CDW gap parameter $\Delta_c=W/\sinh(2W/u_p)$.

For the superconducting phase the calculations are also of the BCS type. Since there are two Cooper-pair order parameters, namely, the on-site pairing amplitude b_s and the nearest-neighbor pairing amplitude b_e, the gap equation is now a 2×2 matrix equation. The transition temperature T_c is obtained from the condition that the determinant of the matrix

$$\tilde{\mathrm{M}}=\left[1-\frac{1}{2N}\sum_k{}'\frac{\tanh(\bar{\epsilon}_{\mathbf{k}}+\bar{\mu})}{(\bar{\epsilon}_{\mathbf{k}}+\bar{\mu})}\begin{pmatrix}U & -Vz\gamma_{\mathbf{k}}\\ U\gamma_{\mathbf{k}} & -Vz\gamma_{\mathbf{k}}^2\end{pmatrix}\right] \quad (5)$$

should vanish at this temperature (Appendix C); here 1 is the 2×2 unit matrix. Note that, in mean-field theory, the maximum superconducting T_c occurs at the bicritical point.

B. The cooperon bound state in the CDW phase and elementary excitations

In the large-U limit a pseudospin model emerges naturally from the negative-U, extended-Hubbard model[2,5] and the well-separated optical and transport gaps[6] can be explained by identifying the optical gap with the pair-breaking energy or the energy for breaking up the spin and the transport gap with the pseudospin-wave gap in the CDW semiconducting phase. Even in the intermediate-U case the CDW phase continues to show two well-separated gaps, whose physics is understood as follows: Our mean-field theory yields quasiparticle valence and conduction bands [Fig. 2(a)] with a gap separating them (along the entire noninteracting Fermi surface in k space). At half filling (i.e., pure $BaBiO_3$) this system is insulating in the ground state, since the valence band is full and the conduction band is empty. If we put two electrons into the conduction band, they still feel a residual attraction U (modified by appropriate coherence factors), so they form a bound state (a cooperon) whose energy lies within the gap in the two-particle excitation spectrum [Fig. 2(b)]. Two holes in the valence band form a similar bound state. These bound states form provided the source of the negative U is electronic[4] and not phonon mediated,[3] since U must remain attractive over energy scales larger than the charge-density-wave gap Δ_c ($\simeq 1$ eV, as measured from the Fermi level) in order to produce a state with binding energy $\simeq\Delta_c$. Clearly, the energy required for exciting these bound pairs or cooperons is that needed for creating two free quasiparticles, namely $2\Delta_c$, *minus* their binding energy E_B. This difference, which is always less than $2\Delta_c$, is shown in Fig. 2(b). Note that such a bound state is always present no matter how weak the attraction U is. We find that, for large U and small V, the cooperon excitation energy is of order zV, which is rather small. The cooperons are the lowest-lying current- and charge-carrying excitations of the CDW ground state. Furthermore they are extended states, characterized by a center-of-mass momentum. Thus, in this model, the cooperons are expected to determine the transport properties of the CDW state. For example, the activation gap for electrical transport is $(2\Delta_c-E_B)$. However, optical experiments which excite single particles across the CDW gap, measure the gap Δ_c.

The actual calculation of the pair spectrum is somewhat complicated, and proceeds as follows. The propagation of a pair of electrons (or holes) with total momentum q and energy ν is described by the function $\chi_{p,ij;i'j'}(\mathbf{q},\nu)$ given by

$$\chi_{p,ij;i'j'}(\mathbf{q},\nu)=\frac{1}{2\pi N^2}\int_{-\infty}^{+\infty}d\tau\exp(i\nu\tau)\sum_{\mathbf{k},\mathbf{k}'}{}'\langle T_\tau[c_{\mathbf{k}+\mathbf{q}\uparrow,i'}(\tau)c_{-\mathbf{k}\downarrow,j'}(\tau)c^\dagger_{\mathbf{k}'+q\uparrow,i}(0)c^\dagger_{-\mathbf{k}'\downarrow,j}(0)]\rangle\ ,$$

where T_τ indicates time ordering, i,j, etc., are band indices (in the CDW ground state there are two bands), the subscript p stands for pairing, and the expectation value is calculated in the interacting ground state, since we restrict ourselves to $T=0$. A pole in the pair susceptibility (at wave vector $\mathbf{q}=0$) below the bottom of the continuum of the two-particle excitation spectrum [which starts at $2\Delta_c$ in Fig. 2(b)] indicates a two-particle bound state of zero total momentum.

We calculate this pair susceptibility in a ladder approximation (Appendix D), in the presence of a CDW background and starting from a negative-U, extended Hubbard model at half filling. The ladder describes the repeated scattering of pairs by the local attractive two-body potential (Fig. 3). Thus we obtain the two-particle (two-hole) excitation spectrum and thence the location of the cooperon bound state (cf., the t-matrix calculation of Migdal[27] for superconductors). If $zV<\Delta_c$ (which is the case for the barium bismuthates since $\Delta_c\simeq 1$ eV), the two-particle bound state falls within the gap of the two-particle spectrum [Fig. 2(b)] and, for any nonzero V, it lies above the chemical potential (from which all energies are measured).

The bound-state energy we calculate here evolves into the pseudospin-wave gap of the large-U model, where the pseudospin-wave spectrum is obtained from the poles of

$$\mathcal{G}^{+-}(\mathbf{q},\nu)=\frac{1}{2\pi}\int_{-\infty}^{+\infty}d\tau\exp(i\nu\tau)\langle T_\tau[S^+_{\mathbf{q}}(\tau)S^-_{\mathbf{q}}]\rangle\ ,$$

where S^+ is the pseudospin raising operator. $\mathcal{G}^{\pm}$, can be written in terms of the fermion operators $c_{k\alpha}$ by using $S^+_{\mathbf{q}}=1/N\sum_{\mathbf{k}}c^\dagger_{\mathbf{k}+\mathbf{q}\uparrow}c^\dagger_{\mathbf{k},\downarrow}$, and shown to be equivalent to the pair susceptibility defined above. It is interesting that the excitation spectrum we calculate here evolves into the RPA pseudospin-wave spectrum we calculated directly in the large-U limit[2,5] (for it is not evident that the approximations used in the two cases are equivalent in all respects).

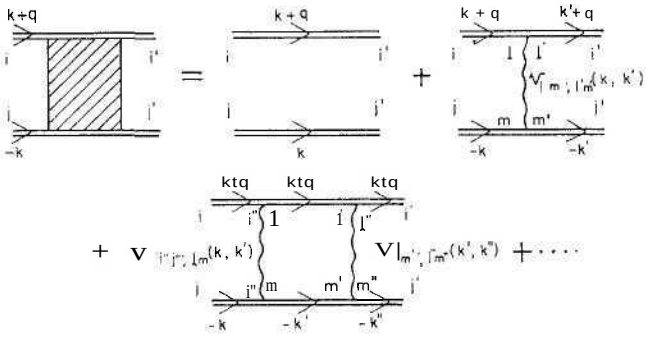

FIG. 3. The diagrammatic representation of the ladder series for the pair susceptibility in the mean-field CDW state. Double lines denote mean-field, single-particle Green function in the CDW state and the wavy line denotes the interaction $V_{ij;i'j'}(\mathbf{k},\mathbf{k}')$.

The Cooper-pair problem in a CDW background, with on-site *and* nearest-neighbor interactions is complicated, for there are the two CDW split bands, with the electronic states of interest being, in general, superpositions of these band eigenstates. However, with a separable interparticle potential, the Cooper problem is exactly solvable. Hence we rewrite the nearest-neighbor interaction V as a sum of separable terms. (The on-site term is trivially separable, since it has no momentum dependence.) This finally leads to a 14×14 matrix secular equation, a generalization of the one-band, Cooper-instability equation (see Appendix D). As in the conventional Cooper problem with an attractive U, a two-particle bound state splits

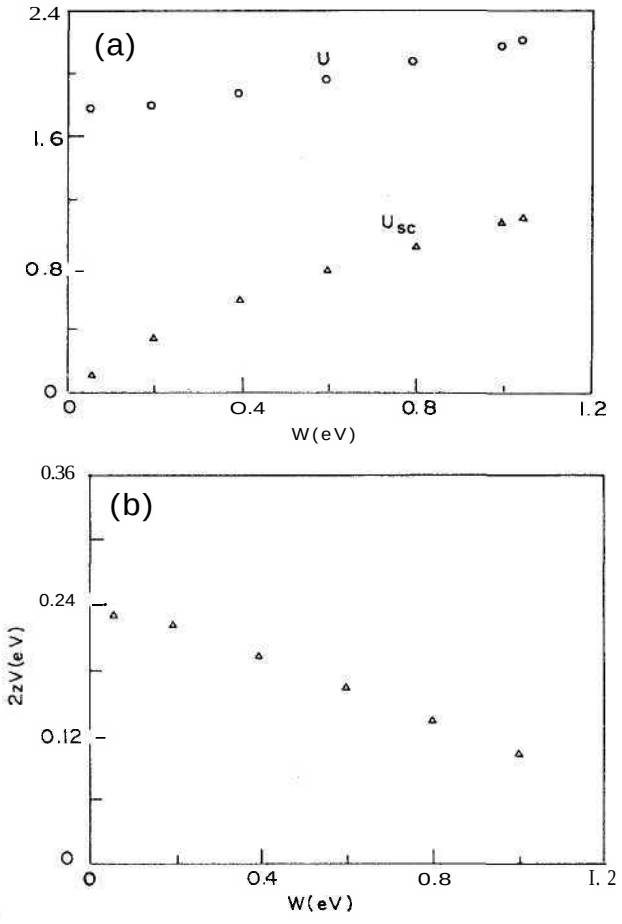

FIG. 4. (a) The bare and the screened, on-site Coulomb interactions (empty circles and triangles, respectively) as functions of half the band width. The screening mechanism is explained in the text. (b) The extended Coulomb term $V(X2z,z=6$ for a simple-cubic lattice) as a function of half the bandwidth. The condition we used to obtain this graph is that the bound-state energy should be equal to the transport gap (see the text). Note that in the bandwidth $\rightarrow 0$ limit the value of $2zV$ approaches 0.24 eV, the result obtained in the large-U limit (Ref. 2).

off from the two-particle continuum. It should be emphasized that the bound state is characterized by total momentum. It is a spatially extended, current-carrying state, intrinsic to the system, *unlike* the localized nonpropagating state within the band gap, induced by a local impurity potential.

C. Estimates and limits

The energy of the bound state depends on U, V, and zt. In order to fix at least some of our parameter values, we proceed as follows: (1) We set $\Delta_c = 1$ eV, taking the optical gap ($=2\Delta_c$) to be 2 eV for $BaBiO_3$. (We use the mean-field gap equation and a constant density of states, so $\Delta_c = z\tilde{t}/\sinh(2z\tilde{t}/u_p)$, where $u_p = U + 2zV$ and zt is half the bandwidth.) (2) We set the cooperon bound-state energy (measured from the chemical potential) equal to the transport gap of $BaBiO_3$, i.e., 0.24 eV. The values of U (both screened and unscreened, see below) and V given by these two conditions are plotted versus zt in Figs. 4(a) and 4(b). For the potassium-doped system the bandwidth is roughly 1.6 eV from the experimental density of states[9] in the vicinity of the metal-semiconductor transition. This yields $U = 1.9$ eV and $2zV = 0.13$ eV [Figs. 4(a) and 4(b)]. Clearly then we must consider the intermediate-U and not the large-U case. The main results obtained from the above calculations are summarized below.

(1) In Fig. 5 we show the values of the interaction parameters obtained from the two conditions described above, for a fixed value of zt, as a function of the bound-state energy. The two-particle bound-state energy goes to zero (relative to the chemical potential) continuously as V approaches zero (Fig. 5). At $V = 0$ there is a gapless, two-particle mode that signals the instability of the CDW state towards superconducting order.

(2) The bound-state energy goes to $2zV$ as $zt \to 0$ [Fig. 4(b)]. In the large-U limit the anisotropy gap is $2zV$, a feature that is reproduced correctly here as $zt \to 0$. Thus our results interpolate smoothly between small- and large-U results for the extended Hubbard model at $T = 0$.

At $\delta = 0$ and F=0, the CDW phase is degenerate[26] with the superconductor because of a continuous pseudospin-rotation symmetry (see above and Ref. 24). The spontaneous breaking of this symmetry should yield a gapless spectrum (in the large-U or pseudospin-model limit this corresponds to $\omega \propto q$ as $q \to 0$ for the isotropic Heisenberg antiferromagnet[28]). In Appendix E we show how we obtain this gapless spectrum from the poles of $\chi_p(\nu, \mathbf{q})$ at $V = 0$ and show how, at large U, we obtain the same spin-wave velocity as we did for the pseudospin model.[2] If $V \neq 0$, the bound state is pushed up from the chemical potential to a finite value (determined by V) and the spectrum acquires a gap.

At half filling and with $V = 0$, the negative-U Hubbard model can be transformed into a positive-U model by a particle-hole transformation on one of the spin species and a subsequent rotation by π of the spins on one of the sublattices. (This rotation is necessary because the degenerate particle and hole states are separated in momentum space by a zone-corner wave vector for a tight-binding model on a bipartite lattice.) Thus (for F = 0) the pseudospin-wave spectrum obtained for the negative-U model from this particle-particle susceptibility in its CDW phase should be identical to the corresponding spin-wave spectrum for the positive-U model obtained from the spin susceptibility in the particle-hole channel and in its spin-density-wave phase, which has been studied earlier.[29,30] Indeed our results for $V = 0$ (transformed as described above) are the same as those of Schrieffer, Wen, and Zhang, Kostyrko,[29] and Singh and Tesanović[30] for the positive-U model. (We agree completely with the second set of authors; the former have missed a factor of $\frac{1}{2}$.) The spin-wave velocity[28] that we obtain is $v_s = \sqrt{2}J$, where $J = 4\tilde{t}^2/U$ and the spin-wave spectrum is given by $\omega^2 = 4J^2(1 - \gamma_{\mathbf{q}}^2)$, with $\gamma_{\mathbf{q}} = 1/z \sum_{\mathbf{a}} e^{-i\mathbf{a}\cdot\mathbf{q}}$, where $\{\mathbf{a}\}$ are the nearest-neighbor lattice vectors.

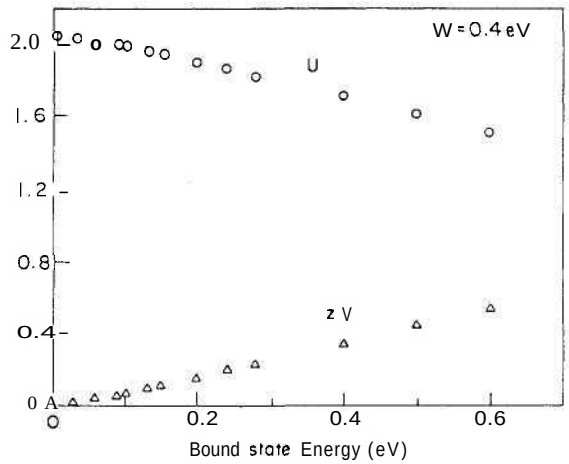

FIG. 5. The Coulomb interactions U and zV as functions of the bound-state energy. This graph is obtained with the condition that the CDW gap parameter is half the optical gap of $BaBiO_3$ (i.e., 1 eV). Note that V goes to zero as the bound-state energy approaches zero.

D. Optical properties

We also calculate (Appendix F) the optical conductivity in the single- and two-particle channels by using the Kubo formula and the RPA. For simplicity and the purposes of illustration, we do this calculation in the large-U limit. The resulting optical conductivity is shown in Fig. 6. These calculations were done at a moderately large $U \simeq 2zt$ and with reasonable values of the rest of the parameters (for the bismuthates). We assume that scattering yields the same phenomenological relaxation time for both the channels (thus the 8 functions that appear in our calculation in Appendix F broaden into Lorentzians). Note that, even at this level of approximation, the peak in the two-particle channel (at 0.24 eV) is nearly a factor of 10 smaller than the one-particle peak (at 2 eV). The main reason for this suppression of the two-particle peak is that the cooperon current (vertex) has an extra factor of t/U with respect to the single-particle vertex, because it arises out of second-order hopping (in t_{ij}) and the ratio $(t/U)^2 \lesssim 10^{-1}$. Thus the optical-absorption peak at the transport gap is indeed intrinsically much weaker than

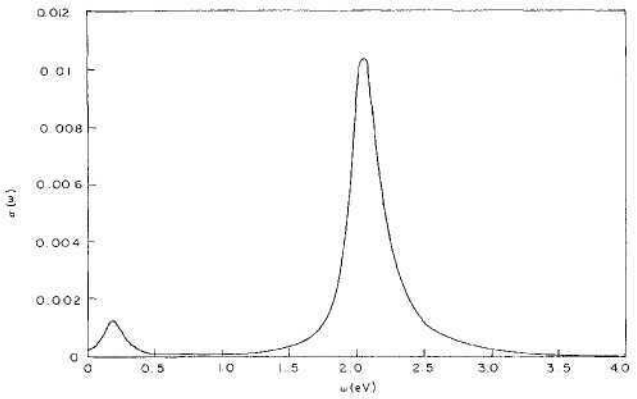

FIG. 6. The optical conductivity (in arbitrary units) in the large-U limit using the random-phase approximation plotted as a function of frequency. The parameter values chosen are zt = \ eV, $U=2$ eV, and $2zV=0.1$ eV. We have used the same phenomenological broadening ($\Gamma=0.09$ eV) for the two channels. Note that the two-particle absorption peak (at 0.24 eV) is down by a factor of 9 compared to that in the single-particle channel (at 2 eV).

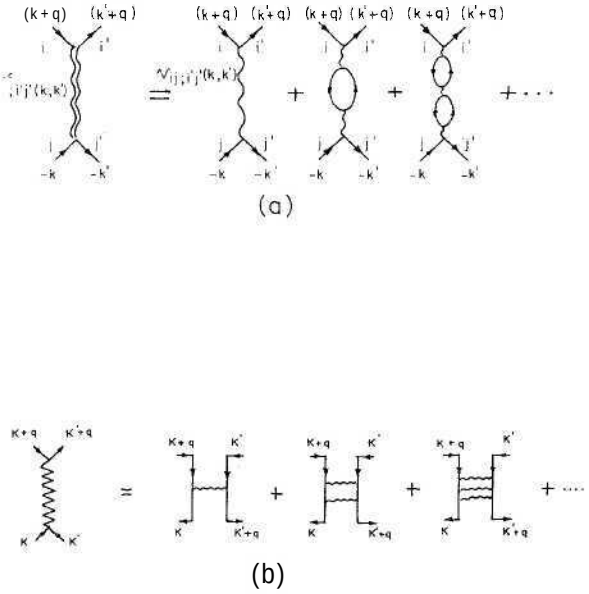

FIG. 7. A diagrammatic representation of the screening (in RPA) of the particle-particle and particle-hole vertices. Note that the particle-particle vertex (a) is screened by the particle-hole excitations whereas the particle-hole vertex (b) is screened by particle-particle processes.

the one at the optical gap. It is also possible that there are other nonperturbative, orthogonality effects that exponentially reduce the optical absorption at the transport gap, which is why it does not show up at all in optical-conductivity experiments.

III. COMPARISON WITH EXPERIMENT

We return now to the barium bismuthates and compare our results with experiments. However, we cannot naively use our estimates for the values of U and V to calculate the superconducting and CDW transition temperatures for the following reasons: Our estimates of U and V have been made at the extreme insulating limit of $BaBiO_3$, whereas superconductivity and the metal-semiconductor transition occur after significant doping ($\delta \simeq 0.4$ for the potassium-doped system). We must, therefore, try to incorporate the effects of metallic screening on the strength of the Coulomb interaction. Also it is conceivable that, at high doping levels, as the system moves towards the metallic side and the lattice distorts and the charge-disproportionated, highly ionized Bi configurations begin to disappear, the mechanism,[4] which leads to the attractive interaction, gets suppressed. At this stage it is difficult to account for these effects as we do not have a first-principles theory for the negative value of U. Further, we have completely neglected the effect of disorder. It is clear from the persistence of the insulating state with doping, for example, that disorder effects are very important (see Sec. IV for further discussion).

In order to account for some of the physical processes that occur on doping, we have included the effect of metallic screening at the simplest level via the RPA (the screening diagrams Figs. 7(a) and 7(b) represent repeated excitations of particle-hole or particle-particle pairs, as the case may be, out of the Fermi sea). Screening operates in both particle-particle and particle-hole channels. Hence the effective interactions responsible for CDW ordering and superconductivity are *both* reduced. We use the RPA to calculate the t matrix and write the effective (screened) interaction as $v_{sc}(\mathbf{q})=v(\mathbf{q})/[1-v(\mathbf{q})\chi_0(\mathbf{q})]$, where v is the bare interaction and $\chi_0(\mathbf{q})$ is the appropriate, bare susceptibility (particle-particle or particle-hole). Since the particle-hole susceptibility at $q=Q$ is the same as the particle-particle susceptibility at $q=0$, at the simplest level, we can replace χ_0 by the density of states $N(0)$ at the Fermi level and get the effective screened interaction governing the CDW or superconducting transitions. For $N(0)$ we use the experimental value at the metal-semiconductor boundary of the potassium-doped system. Note that we have used screening[31] for the on-site Coulomb term only, as a calculation of the t matrix for the momentum-dependent V term is rather complicated. Since the values of V we are interested in are quite low (see below) compared to U, we feel it is justifiable to neglect the screening corrections to V.

In Figs. 8(a) and 8(b) we plot the superconducting and CDW transition temperatures [Eqs. (4) and (5)] as functions of the bandwidth (with both bare and screened interactions). The results of our detailed mean-field calculation (Appendix C) are shown in Fig. 9 (where the parameter values are the same as in Fig. Kb), but the two-phase coexistence region is now shown). V has a negligible effect on T_c in the range of interactions that we are interested in. This can be seen from the dashed line in Fig. 9 for the superconductor-nonordered metal phase boundary with $V=0$. [Indeed V has no effect on the superconducting T_c if 8 vanishes; Eq. (C6), Appendix C.] Our values for the superconducting and CDW transition

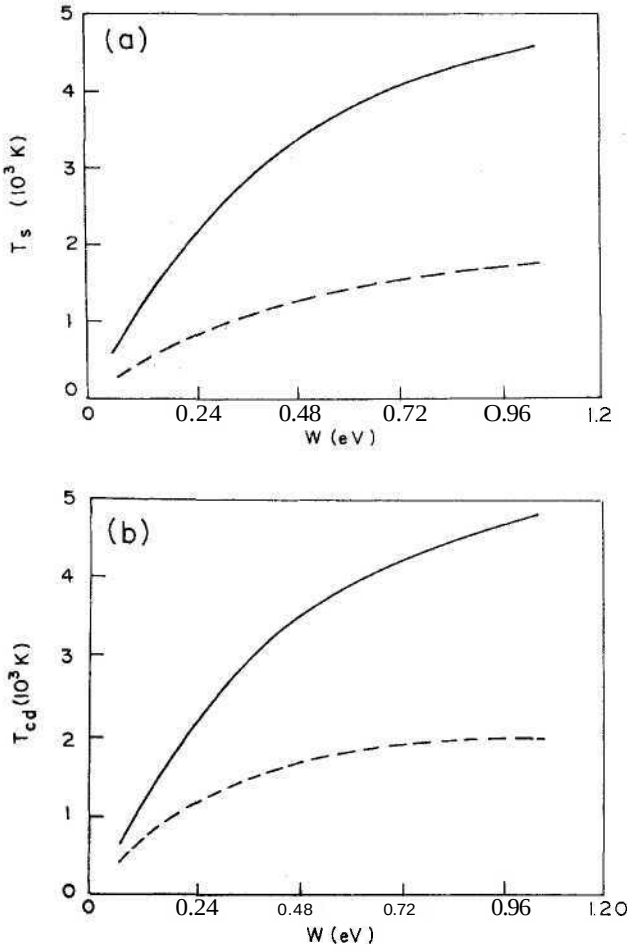

FIG. 8. (a) The superconducting and (b) the CDW transition temperatures with bare and screened onsite Coulomb interactions, obtained from a BCS formula (see text) as a function of (half) the bandwidth. The lower graph in each case is obtained with the screened interactions.

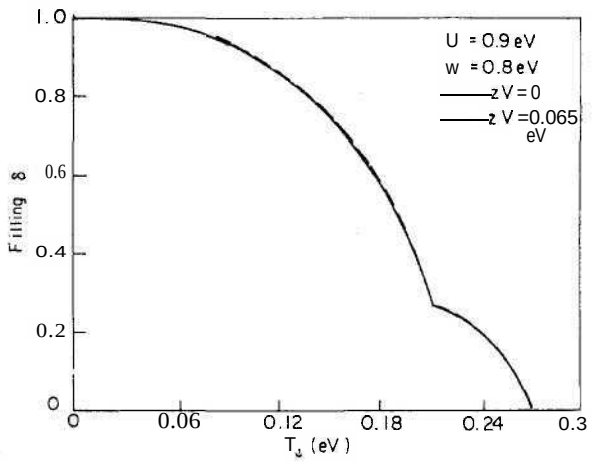

FIG. 9. The superconductor-nonordered phase boundary with the same parameters as in Fig. Kb) (we do not show the two-phase coexistence regime here). To show that the screening of V does not affect the phase boundary in the range of parameter values we are interested in, we have drawn the phase boundary for $V=0$ (dashed line). Note that this boundary is quite close to the boundary with $2zV=0.13$ eV (this boundary is also continuous).

temperatures, especially the former, are still too high compared to experiments. (The limited data that exist on T_{CD} are[10] in the range 0.06 to 0.0025 eV, for different fillings.) There could be several reasons for this. Even in a clean system, the interaction parameters U and V may decrease on doping because of additional nonlinear screening effects. Also, quantum-fluctuation effects, prominent since both pairing and CDW instabilities are close to each other, must further reduce T_c. Finally, there is the strong effect of disorder; this is clearly indicated by the fact that the superconducting T_c is highest close to the critical disorder, where normal-state resistivities are very large, and, more generally, by the persistence of the insulating phase for very large deviations from half filling.

The effect of disorder is very hard to quantify reliably. An estimate, valid for $BaPb_{1-x}Bi_xO_3$, can be made by assuming simple dilution as follows. Since Bi ions are the source of the local negative U, we replace U by Ux when their concentration is x. This replacement also leads to a deviation $\delta=1-x$ from half filling (at which the system is a CDW). A calculation of the Cooper instability leads to a substantial reduction in the T_c (by an order of magnitude near the bicritical point of Fig. 1), even though our method, a kind of average t-matrix approximation, greatly underestimates the effect of disorder.

In spite of obtaining large transition temperatures, our theory yields many interesting results: (1) We can easily understand why the transport gap is well separated from the optical gap because of the two-particle bound state in the CDW phase (see above). The conductivity is given by $\sigma(\omega)=[n(T)e^{*2}\tau/m^*]/(1-i\omega\tau)$, where m^* is the effective mass of the cooperons, $e^*=2e$ their charge, $n(T)\sim\exp(-E_A/k_BT)$ their number at temperature T, and E_A is the transport gap. Clearly $\sigma(\omega\to0)$ exhibits activated behavior. (2) Our theory obtains various qualitative features of the phase diagrams of these bismuthates. (3) In addition, $2\Delta/k_Bt_c\simeq3.5$, all low-T phases in our model are diamagnetic, and the superconducting coherence length is $\simeq30$ Å, far closer to the experimental value ($\simeq80$ Å) than that predicted by the large-U limit,[2] in which case we have on-site paired electrons. (To obtain the coherence length we have taken the standard mean-field expression and used the observed values of the Fermi velocity.) Since our calculation grossly overestimates the superconducting T_c, it is not surprising that our estimate for the coherence length is somewhat smaller than the experimental value.

IV. CONCLUDING DISCUSSIONS

In this paper and elsewhere[2,5] we have investigated the negative-U, extended Hubbard model for the bismuthate superconductors both in intermediate- and large-U regimes. Our study leads to an understanding of many of the properties of these bismuthates and sharpens certain

questions that remain unanswered.

Perhaps the most important result of our treatment is the detailed theory we provide for the two gaps in the semiconducting phase of these bismuthates. This leads to the identification of the transport gap with the energy of the two-particle bound state and the optical gap with twice the CDW gap. Our calculations also show how this picture of the two gaps is consistent with the inaccessibility of the transport gap in optical-reflectance, photoacoustic, and photoconductivity studies, all of which involve single-particle excitations. Note that *our picture also implies that the semiconducting phase of these bismuthates is unique, with transport properties dominated by the motion of charge-2e bosons* (cooperons).

By fitting our predictions for the gaps to the experimental ones we have estimated the interaction parameters for these bismuthates and used them to calculate other normal-state and superconducting properties. We have also calculated the particle-particle excitation spectrum in the ladder approximation in the CDW phase of model (1); our intermediate-U excitation spectrum evolves smoothly into the pseudospin-wave spectrum expected in the large-U limit.[2]

For typical intermediate values of U and V (i.e., $U \leq 2zt$ and $V < U$) our phase diagram [Fig. 1(a)] has the same qualitative features as the large-U phase diagram,[2,5] and shares many features with the experimental phase diagram. The charge contrast in the CDW phase is lower in the intermediate-U case (in agreement with experiments) relative to the large-U case. Similarly, the intermediate-U superconducting coherence length is enhanced over its large-U limit, in better accord with the experiments.

We have also argued that the processes that give rise to the attractive interaction must be electronic in origin and that these processes must become less and less effective as the system is doped towards the metallic side, so the strength of the attractive interaction must go down in order to produce the experimentally observed superconducting transition temperatures.

Our theory rules out a purely phonon-mediated mechanism for the negative U (unless an alternative explanation can be found for the well-separated optical and transport gaps): A phonon-mediated attraction is necessarily retarded (cutoff at characteristic phonon frequencies $\simeq 100$ K); however, in order to produce the two gaps, the attraction must operate over a range $\simeq 1$ eV. This observation is important in view of the recent observation[10,11] that calculations based on realistic phonon spectra for the bismuthates can produce a rather large superconducting T_c without requiring a very strong electron-phonon coupling strength ($\lambda_{e\text{-}p} \simeq 0.6$–$0.8$) or a large density of states at the Fermi level. We have argued that, at least in the semiconducting phase of these systems, the attraction should have an electronic origin. However, we do not rule out the possibility that this electronic component of the attraction becomes weak as the system is driven towards the metallic side by doping; here the electron-phonon coupling could become important near the superconducting phase.

In a recent paper Liechtenstein *et al.*,[32] have carried out what is perhaps the best band-structure study of $Ba_{1-x}K_xBiO_3$ to date using the LDA and the full linear muffin-tin-orbital method. For $x=0$ they find a lattice instability for a combination of both tilt (u_t) and breathing (u_b) distortions which correctly reproduces the experimentally observed monoclinic structure. For $x=0.5$ they correctly find the cubic phase, with $u_t = u_b = 0$, to be stable.

An interesting point that emerges from this band-structure study is that, when the details are put in, $BaBiO_3$ may have a rather small indirect band gap. (The actual number that we have been able to glean from Fig. 2 of Liechtenstein, *et al.*,[32] roughly 0.025 Ry or 0.34 eV, may not be reliable.) Hence one must consider the possibility that the small transport gap (0.24 eV) reflects this aspect of the band structure. However, optical experiments must be able to see this as a phonon-assisted threshold, starting around 0.68 eV, in order to be consistent with the transport gap. However, all the data that we have seen have thresholds starting at 1 eV. (For recent spectroscopic data see Ref. 40.) If the latter is taken as the indirect gap, the discrepancy with the transport gap is still too large to be understood in conventional terms. (For example, if one were to attribute it to polaronic or bipolaronic effects, as some groups have done,[6,40,41] the resulting Franck-Condon factors would be too large, leading to self-trapped rather than mobile carriers as required by the observed mobilities.) Thus one clearly needs a mechanism of the sort we have been discussing, although for a proper comparison with experimental data and a better estimate of the parameters U and V it seems crucial to include the details of the band structure.

In our theory the carriers responsible for charge transport in the semiconducting phase of these bismuthates are charge-2e bosons (cooperons). Hence an experiment that can pick up the charge of the carriers in this phase would be of great value in verifying our theory. It is well known that, in transport measurements, it is very difficult to determine the charge of a carrier as the electrical conductivity depends on the ratio of the effective charge and the effective mass. At a simple level the following experiments might be able to measure the charges of the carriers in the semiconducting phase of the bismuthates: (1) Stanton and Wilkins[36] show that the noise spectrum of high-field transport in a semiconductor is

$$S(\omega,E) = (ne^{*2}\tau_0)/[1+(\omega\tau_0)^2] \times (A/2L)[k_B T_0/m^* + (e^* E \tau_0/m^*)^2],$$

where E is the external electric field, T_0 is the equilibrium lattice temperature, τ_0 is the phenomenological relaxation time of the charge carrier of effective charge e^* and mass m^*, and A and L are, respectively, the area and length (in the direction of transport) of the sample. If the thermal- and electric-field-dependent components of the noise spectrum could be separated, the above expression for $S(\omega,E)$ would allow one to calculate the charge of the carriers and their effective mass separately. To measure the noise spectrum, however, one must do a very controlled experiment at low temperatures on a pure, single-crystal sample of $BaBiO_3$. (2) A Bohm-Aharanov mea-

surement of the phase change on passing through a magnetic field can, in principle, detect the charge of the carrier. (3) The charge-$2e$ cooperons may also show up in tunneling from a metal to the semiconductor or in Andreev-reflection measurements. (4) It is also possible that the existence of the local on-site attraction can lead to strong fluctuation effects in the metallic phase;[37] these could show up in transport and magnetic properties at temperatures close to T_c. (5) Optical-absorption experiments on optically pumped $BaBiO_3$ or a two-photon absorption experiment might be able to pick up lines corresponding respectively to the breaking or formation of the cooperons. (Photomodulation studies[41] show some evidence of states in the gap, but their interpretation requires detailed modeling, including band-structure effects, which is beyond the scope of this paper.) We believe that such experiments that confirm or rule out this picture of the semiconducting phase of the barium bismuthates would be of great interest, for that would confirm or fuel out the electronic (as opposed to phonon-mediated) origin of the negative U. One should note that such experiments may be difficult to perform and hard to interpret.

Our mean-field phase diagram (Fig. 1) for model (1) does not contain an intermediate phase (with both CDW and superconducting order) unlike the mean-field phase diagram of Micnas and co-workers,[20,21] which is not correct (since it does not allow for first-order phase coexistence between CDW and superconducting phases). In the large-U case Liu and Fisher[23] and Matsuda and Tsuneto[38] have shown that, in mean-field theory, an intermediate phase occurs only when next-nearest-neighbor interactions (extended Coulomb) are included.

The ladder summation we do in the intermediate-U case to calculate $\chi_p(q)$ considers only a small subset of the processes (diagrams) involving two-particle interactions. There are other many-body processes that are probably important in the range of interactions we are considering. Our choice of the ladder approximation was motivated by its physical importance and its simplicity. It is interesting that this, in itself, leads to excitation spectra that evolve smoothly from the intermediate-U case to the pseudospin-wave spectrum expected at large U.[2]

Even though the negative-U extended Hubbard model leads to many appealing results for these bismuthates, it has its limitations. The main shortcomings arise because we neglect electron-phonon interactions, the long-range part of the Coulomb interaction, and disorder effects (charge disorder in the case of $Ba_{1-x}K_xBiO_3$). We comment on these shortcomings below.

The neglect of Coulomb interaction is probably the main reason for one important discrepancy between the experimental phase diagrams[1,10] and our phase diagram (Fig. 1): the former have no two-phase region for $x < 0.4$, unlike the latter. The CDW and superconducting phases have different average Bi occupancies (or charge), so the long-range Coulomb interaction will strongly disfavor any bulk phase separation; instead it might favor the formation of a new phase consisting of a dispersion of globules of superconducting material in a semiconducting (CDW) background. If the background compensating charge (because of K ions) were smeared uniformly, one might expect this dispersion to be a periodic array. However, in the actual system the K ions are distributed randomly, so the dispersion might well be random. Certainly for small deviations from half filling (i.e., $\ll \simeq 1$) one expects a dispersion of superconducting globules (which, in the large-U limit and with small-enough globule sizes, can be thought of as discommensurations[4] inside a CDW background). Such a phase would be semiconducting above a new critical temperature (much lower than the critical temperature for the bulk superconductor) corresponding to the destruction of the phase coherence between the different superconducting globules (a temperature determined by the weak, Josephson coupling between the globules). It is interesting to speculate that the semiconducting region, which extends away from half filling experimentally,[1,10] is such a dispersed phase.

An alternative possibility that one ought to explore, both theoretically and experimentally, even in the nearest-neighbor model (2) and within the mean-field framework, is whether the first-order phase-coexistence region of Fig. l(b) gets replaced by an incommensurate phase, or a succession of commensurate phases.

Next, one should take into account the effects of disorder: In the potassium-doped case, K^{1+} replaces Ba^{2+}. Thus, in addition to one electron being removed from the system (which we have considered in our model), a random Coulomb potential is introduced (K is like a 1^- impurity). In our theory we neglect this random, impurity, Coulomb potential. The effect of randomness is even more serious in lead-doped $BaBiO_3$, since the Pb atoms remove the negative-U Bi centers randomly. Only the simplest studies of the effects of this on CDW ordering have been carried out so far.[3]

Since $BaPbO_3$ is a metal, it is clear that, for a serious study of the entire range of lead doping, the one-band model (2) is inadequate and a more complex, three-band model[2,4] must be studied. Also, the electron-phonon interactions in these systems are strong, so they have to be taken into account much better than has been done so far, especially to understand the structural transitions in these bismuthates. Clearly more detailed experimental and theoretical studies are called for to address these issues.

ACKNOWLEDGMENTS

We would like to thank the University Grants Commission and the Council for Scientific and Industrial Research (India) for support (for work done in India) and the Supercomputer Education and Research Centre, Indian Institute of Science for providing computer resources. We also thank P. W. Anderson, G. Baskaran, B. Batlogg, R. N. Bhatt, S. Bhattacharya, H. R. Chandrasekhar, P. Coleman, R. Collins, D. L. Cox, S. Dattagupta, C. Dasgupta, J. Gopalakrishnan, E. S. Hellman, T. Hsu, C. Jayaprakash, N. Kumar, P. Lederer, D. H. Lee, S. Ramaswamy, B. S. Shastry, C. N. R. Rao, T. M. Rice, S. Sachdev, C. M. Varma, P. Wolff, N. Wingreen, and S. C. Zhang for stimulating discussions. One of us (R.P.)

would like to thank The Ohio State University for hospitality. This paper was supported in part by the U.S. Department of Energy (Contract No. DE-F-G02-88ER13916AOOO). T.V.R. thanks IFCPAR for support through research project No. 408-2.

APPENDIX A: THE HARTREE-FOCK APPROXIMATION FOR THE NEGATIVE-U, EXTENDED HUBBARD MODEL, AND THE MEAN-FIELD FREE ENERGY

We start from the Hamiltonian (Sec. II)

$$H=-t\sum_{\langle ij\rangle\sigma}c_{i\sigma}^{\dagger}c_{j\sigma}-\frac{U}{2}\sum_{i\sigma}n_{i\sigma}n_{i,-\sigma}+\frac{V}{2}\sum_{\langle ij\rangle\sigma\sigma'}n_{i\sigma}n_{j\sigma'}-\mu\sum_{i\sigma}n_{i\sigma}\ , \tag{AD}$$

where $U>0$, and use the order parameters of Eq. (2).

We use a standard mean-field decoupling (i.e., for two operators A and $\hat{B}$ we write $\hat{A}\hat{B}\rightarrow\langle\hat{A}\rangle\hat{B}+\langle\hat{B}\rangle\hat{A}-\langle\hat{A}\rangle\langle\hat{B}\rangle$) to obtain the mean-field Hamiltonian

$$\begin{aligned}H_{\rm mf}=&-\sum_{\mathbf{k}\sigma}(\bar{\epsilon}_{\mathbf{k}}+\bar{\mu})c_{\mathbf{k}\sigma}^{\dagger}c_{\mathbf{k}\sigma}-\Delta_c\sum_{\mathbf{k}\sigma}c_{\mathbf{k}+Q\sigma}^{\dagger}c_{\mathbf{k}\sigma}\\&-\sum_{\mathbf{k}}\Delta_s(\mathbf{k})(c_{-\mathbf{k}\downarrow}c_{\mathbf{k}\uparrow}+c_{\mathbf{k}\uparrow}^{\dagger}c_{-\mathbf{k}\downarrow}^{\dagger})\\&+N\left[Ub_s^2-Vzb_e^2+\frac{1}{4}n^2u_m+\frac{1}{4}b_c^2u_p+\frac{1}{4}VzC_0^2\right],\end{aligned} \tag{A2}$$

where the symbols have been defined after Eq. (3).

In terms of the operators $c_{\mathbf{k}\sigma}$ defined in Fourier space, the principal order parameters are $b_c=\sum_{\mathbf{k},\sigma}\langle c_{\mathbf{k}+\mathbf{Q}\sigma}^{\dagger}c_{\mathbf{k}\sigma}\rangle$, $b_s=\sum_{\mathbf{k}}\langle c_{-\mathbf{k}\downarrow}c_{\mathbf{k}\uparrow}\rangle$, and $b_e=\sum_{\mathbf{k}}\gamma_{\mathbf{k}}\langle c_{-\mathbf{k}\downarrow}c_{\mathbf{k}\uparrow}\rangle$.

The mean-field Hamiltonian $H_{\rm mf}(2)$ can be written in the form:

$$H_{\rm mf}=\sum_{\mathbf{k}}{}'\psi_{\mathbf{k}}^{\dagger}\tilde{H}_{\mathbf{k}}\psi_{\mathbf{k}}-\bar{\mu}N+\text{const}\ , \tag{A3}$$

by using the Nambu representation

$$\psi_{\mathbf{k}}\equiv\begin{pmatrix}c_{\mathbf{k}\uparrow}\\c_{-\mathbf{k}\downarrow}^{\dagger}\\c_{\mathbf{k}+\mathbf{Q}\uparrow}\\c_{-\mathbf{k}-\mathbf{Q}\downarrow}^{\dagger}\end{pmatrix}. \tag{A4}$$

The const in Eq. (A3) comes from the term inside square brackets in Eq. (A2), the prime over the summation indicates that k is restricted to half the Brillouin zone, and

$$\tilde{H}_{\mathbf{k}}=\begin{pmatrix}-\bar{\mu}-\bar{\epsilon}_{\mathbf{k}}&-\Delta_s(\mathbf{k})&-\Delta_c&0\\-\Delta_s(\mathbf{k})&\bar{\mu}+\bar{\epsilon}_{\mathbf{k}}&0&-\Delta_c\\-\Delta_c&0&-\bar{\mu}+\bar{\epsilon}_{\mathbf{k}}&-\Delta_s(\mathbf{k}+\mathbf{Q})\\0&-\Delta_c&-\Delta_s(\mathbf{k}+\mathbf{Q})&\bar{\mu}-\bar{\epsilon}_{\mathbf{k}}\end{pmatrix}, \tag{A5}$$

which can be diagonalized easily. Its four eigenvalues are $\pm E_{\mathbf{k}}^{\pm}$, where

$$E_{\mathbf{k}}^{\pm}=[R_{\mathbf{k}}\pm 2P_{\mathbf{k}}]^{1/2}\ , \tag{A6}$$

$$R_{\mathbf{k}}\equiv\Delta_c^2+U^2b_s^2+V^2z^2b_e^2\gamma_{\mathbf{k}}^2+\bar{\mu}^2+\bar{\epsilon}_{\mathbf{k}}^2\ , \tag{A7}$$

and

$$P_{\mathbf{k}}\equiv[(Ub_sVz\gamma_{\mathbf{k}}b_e+\bar{\mu}\bar{\epsilon}_{\mathbf{k}})^2+\Delta_c^2(u^2b_s^2+\bar{\mu}^2)]^{1/2}\ . \tag{A8}$$

With these four eigenvalues the mean-field free energy per site, $f=-(1/N\beta)\ln\Xi(\mu,T)$, where $\mathrm{E}\equiv\mathrm{Tr}e^{-\beta H_{\rm mf}}$ is the grand partition function,

$$f=-\frac{1}{N\beta}\ln\prod_{\mathbf{k}\alpha}{}'\{1+e^{-\beta E_{\mathbf{k}}^{\alpha}}\}+\text{const}\ , \tag{A9}$$

where $a=1\cdots 4$ refer to the four eigenvalues and the prime over the product indicates that k is restricted to half the Brillouin zone. Finally

$$\begin{aligned}f=&-\frac{1}{N\beta}\sum_{\mathbf{k}}{}'\left[\ln\cosh^2\left(\frac{\beta E_{-}^{+}}{2}\right)+\ln\cosh^2\left(\frac{\beta E_{\mathbf{k}}^{-}}{2}\right)+4\ln 2\right]\\&+Ub_s^2-Vzb_e^2+\frac{1}{4}n^2u_m+\frac{\Delta_c^2}{u_p}+\frac{1}{4}zVC_0^2+\bar{\mu}(n-1)\ .\end{aligned} \tag{A10}$$

APPENDIX B: SELF-CONSISTENCY EQUATIONS FOR THE ORDER PARAMETERS

The equations for the order parameters follow from the minimization of / [Eq. (A10)] with respect to the order parameters. Hence b_s is obtained from the equation $\partial f/\partial b_s=0$ which yields

$$Ub_s=\frac{1}{2N}\sum_{\mathbf{k}}{}'\left[\tanh\left(\frac{\beta E_{\mathbf{k}}^{+}}{2}\right)g_{\mathbf{k},b_s}^{+}+\tanh\left(\frac{\beta E_{\mathbf{k}}^{-}}{2}\right)g_{\mathbf{k},b_s}^{-}\right], \tag{B1}$$

where

$$\begin{aligned}g_{\mathbf{k},b_s}^{\pm}&=\frac{\partial E_{\mathbf{k}}^{\pm}}{\partial b_s}\\&=\frac{1}{E_{\mathbf{k}}^{\pm}}\left[U^2b_s\pm\frac{1}{P_{\mathbf{k}}}(U^2b_sb_e^2\tilde{V}_{\mathbf{k}}^2+U\bar{\mu}\bar{\epsilon}_{\mathbf{k}}\tilde{V}_{\mathbf{k}}b_e+U^2\Delta_c^2b_s)\right]\end{aligned}$$

are coherence factors and $\tilde{V}_{\mathbf{k}}\equiv zV\gamma_{\mathbf{k}}$.

Equations for the other order parameters Δ_c, b_s, and C_0 follow similarly:

$$zVb_e=-\frac{1}{2N}\sum_{\mathbf{k}}{}'\left[\tanh\left(\frac{\beta E_{\mathbf{k}}^{+}}{2}\right)g_{\mathbf{k},b_e}^{+}+\tanh\left(\frac{\beta E_{\mathbf{k}}^{-}}{2}\right)g_{\mathbf{k},b_e}^{-}\right], \tag{B2}$$

where

$$g^{\pm}_{\mathbf{k},b_e}=\frac{\partial E^{\pm}_{\mathbf{k}}}{\partial b_s}=\frac{1}{E^{\pm}_{\mathbf{k}}}\left[\tilde{V}^2_{\mathbf{k}}b_e\pm\frac{1}{P_{\mathbf{k}}}(U^2b_eb_s^2\tilde{V}^2_{\mathbf{k}}+U\bar{\mu}\tilde{\epsilon}_{\mathbf{k}}\tilde{V}_{\mathbf{k}}b_s)\right]. \quad \text{(B3)}$$

One also has

$$1/u_p=\frac{1}{2N}\sum_{\mathbf{k}}{}'\left[\frac{1}{E^{+}_{\mathbf{k}}}\left[1+\frac{(Ub_s)^2+\bar{\mu}^2}{P_{\mathbf{k}}}\right]\tanh\frac{\beta E^{+}_{\mathbf{k}}}{2}+\frac{1}{E^{-}_{\mathbf{k}}}\left[1-\frac{(Ub_s)^2+\bar{\mu}^2}{P_{\mathbf{k}}}\right]\tanh\frac{\beta E^{-}_{\mathbf{k}}}{2}\right]; \quad \text{(B4)}$$

and

$$zVC_0=\frac{1}{2N}\sum_{\mathbf{k}}{}'\left[\tanh\left[\frac{\beta E^{+}_{\mathbf{k}}}{2}\right]g^{+}_{\mathbf{k},C_0}+\tanh\left[\frac{\beta E^{-}_{\mathbf{k}}}{2}\right]g^{-}_{\mathbf{k},C_0}\right], \quad \text{(B5)}$$

where

$$g^{\pm}_{\mathbf{k},C_0}=\frac{\partial E^{\pm}_{\mathbf{k}}}{\partial C_0}=\frac{V}{E^{\pm}_{\mathbf{k}}}\left[\tilde{\epsilon}^2_{\mathbf{k}}/\tilde{t}\pm\frac{1}{P_{\mathbf{k}}}\bar{\mu}z\gamma_{\mathbf{k}}(Ub_eb_s\tilde{V}_{\mathbf{k}}+\bar{\mu}\tilde{\epsilon}_{\mathbf{k}})\right]. \quad \text{(B6)}$$

The filling is determined by the condition $\delta=-\partial f/\partial\bar{\mu}$ and we obtain

$$\delta=\frac{1}{2N}\sum_{\mathbf{k}}{}'\left[\tanh\left[\frac{\beta E^{+}_{\mathbf{k}}}{2}\right]h^{+}_{\mathbf{k},\bar{\mu}}+\tanh\left[\frac{\beta E^{-}_{\mathbf{k}}}{2}\right]h^{-}_{\mathbf{k},\bar{\mu}}\right], \quad \text{(B7)}$$

where $\delta=n-1$ and $h^{\pm}_{\mathbf{k},\bar{\mu}}=\partial E^{\pm}_{\mathbf{k}}/\partial\bar{\mu}$.

APPENDIX C: THE MEAN-FIELD PHASE BOUNDARIES

1. The charge density wave-nonordered metal (CDW-NO) phase boundary

The four energy eigenvalues [Eqs. (A6)-(A8)] reduce to two sets of doubly degenerate eigenvalues in the CDW phase ($b_s=b_e=0$) given by

$$E_{\mathbf{k}}=-\mu\pm\sqrt{\tilde{\epsilon}^2_{\mathbf{k}}+\Delta_c^2}\,. \quad \text{(CD}$$

At the phase boundary between CDW and NO phases, as T rises from below towards T_{CD} (the transition temperature between CDW and NO), $\Delta_c\to 0$. Hence to obtain T_{CD} as a function of δ we consider the self-consistency equation (Appendix B) in this limit.

When $b_s=b_e=0$, the self-consistency equation (B4) for Δ_c becomes (with $\Delta_c=0$)

$$\frac{1}{u_p}=\frac{1}{2}\int_{-W}^{+W}\rho(\epsilon)\frac{\tanh[(1/2)\beta_{CD}(\epsilon-\bar{\mu})]}{\epsilon}d\epsilon, \quad \text{(C2)}$$

where W is half the width of the (noninteracting) single-particle band and $\rho(\epsilon)$ is the corresponding density of states. (Note that this equation gives the BCS expression for the transition temperature at half filling, i.e., at $\bar{\mu}=0$ and for a constant density of states.) From Eq. (B7) we get, in the CDW phase,

$$\delta=\frac{1}{2}\int_{-W}^{+W}\left[\tanh\frac{\beta}{2}(R_\epsilon-\bar{\mu})-\tanh\frac{\beta}{2}(R_\epsilon+\bar{\mu})\right]p(e)de\,, \quad \text{(C3)}$$

where $R_\epsilon=\sqrt{\epsilon^2+\Delta_c^2}$.

These integrals can be evaluated analytically if we approximate $p(e)$ by a constant density of states. In three dimensions such an approximation is known to give fairly good results. We take $\rho(\epsilon)=1/2W$, so that the normalization condition $\int_{-W}^{+W}\rho(\epsilon)d\epsilon=1$ is satisfied. Then the above equation for δ gives (with $\Delta_c=0$ at the phase boundary)

$$e^{-PC_D W\delta}=\frac{\cosh\beta_{CD}(\bar{\mu}+W)/2}{\cosh\beta_{CD}(\bar{\mu}-W)/2}\,, \quad \text{(C4)}$$

where $\beta_{CD}=1/T_{CD}$. Straightforward manipulations with Eq. (C4) give the chemical potential in terms of T_{CD} and δ:

$$\bar{\mu}=W+T_{CD}\ln\left[\frac{1-e^{(1+\delta)W/T_{CD}}}{e^{(1-\delta)W/T_{CD}}-1}\right]. \quad \text{(C5)}$$

Hence to determine T_{CD} as a function of δ (or $\bar{\mu}$) we choose a value of δ, substitute for $\bar{\mu}$ from Eq. (C5) into Eq. (C2), and obtain T_{CD} by numerically evaluating the resulting integral.

2. Superconductor-nonordered (SS-NO) phase boundary

In the superconducting phase ($\Delta_c=0, b_s\neq 0$, and $b_e\neq 0$) we again get two doubly degenerate eigenvalues:

$$E_{\mathbf{k}}=\sqrt{(\tilde{\epsilon}_{\mathbf{k}}+\bar{\mu})^2+(Ub_s-Vb_ez\gamma_{\mathbf{k}})^2}\,.$$

As for the CDW-NO phase boundary, we obtain Eq. (C5) for $\bar{\mu}$ as a function of δ, with T_{CD} replaced by T_{SS}, the superconductor-nonordered transition temperature. The self-consistency equations for b_s and b_e can, in this case, be written as a 2 X 2 matrix equation:

$$\begin{bmatrix}b_s\\ b_e\end{bmatrix}=\frac{1}{2N}\sum_{\mathbf{k}}{}'\frac{[1-2f(E_{\mathbf{k}})]}{E_{\mathbf{k}}}\begin{bmatrix}U & -Vz\gamma_{\mathbf{k}}\\ U\gamma_{\mathbf{k}} & -Vz\gamma^2_{\mathbf{k}}\end{bmatrix}\begin{bmatrix}b_s\\ b_e\end{bmatrix}, \quad \text{(C6)}$$

and the SS-NO transition temperature can be obtained from the pairing-instability condition, i.e., it is the temperature at which the matrix

$$\tilde{M}\equiv\left[1-\frac{1}{2N}\sum_{\mathbf{k}}{}'\frac{\tanh(\tilde{\epsilon}_{\mathbf{k}}+\bar{\mu})/2T}{(\tilde{\epsilon}_{\mathbf{k}}+\bar{\mu})}\begin{bmatrix}U & -Vz\gamma_{\mathbf{k}}\\ U\gamma_{\mathbf{k}} & -Vz\gamma^2_{\mathbf{k}}\end{bmatrix}\right] \quad \text{(CD}$$

has a vanishing determinant (1 denotes a 2 X 2 unit matrix). This is equivalent to finding the temperature at which the largest eigenvalue of this matrix becomes zero (in the nonordered phase, all the eigenvalues of this matrix are negative). As for the **CDW-NO** phase boundary, we choose a value of 8, determine $\bar{\mu}$ from the analog of Eq. (C5), and obtain T_{SS} from Eq. (C7) (we use a constant density of states as above). The **CDW-SS** boundary, being first order, must be obtained numerically by equating the free energies of these two phases.

APPENDIX D: THE PAIR SUSCEPTIBILITY AND THE COOPERON BOUND STATE IN THE CDW PHASE

Here we calculate the two-particle susceptibility when the system is in the CDW ground state using the ladder approximation. In Sec. D 1 we briefly discuss the quasiparticle excitations. We use these in Sec. D 2 to calculate the pair susceptibility and, from its poles, the cooperon bound-state energies.

1. Quasiparticles in the mean-field CDW state

In the absence of superconducting order ($b_s = b_e = 0$) the mean-field Hamiltonian is (Appendix A)

$$H_{\mathrm{mf}}=\sum_{\sigma}\psi^{\dagger}_{\mathbf{k}\sigma}\mathcal{H}_{\mathbf{k}}\psi_{\mathbf{k}\sigma}+\mathrm{const}\ , \tag{D1}$$

where $\psi_{\mathbf{k}\sigma}=(c_{\mathbf{k}\sigma}c_{\mathbf{k}+\mathbf{Q}\sigma})$,

$$\mathcal{H}_{\mathbf{k}}=\bar{\epsilon}_{\mathbf{k}}\sigma_3-\Delta_c\sigma_1-\bar{\mu}1 \tag{D2}$$

is a 2×2 matrix, σ_1 and σ_3 are the first and third **Pauli** matrices, respectively, 1 is the unit matrix, and Δ_c is the CDW gap parameter. If we introduce the unitary transformation

$$\begin{aligned}\alpha_{\mathbf{k}}&=\cos\theta_{\mathbf{k}}c_{\mathbf{k}}-\sin\theta_{\mathbf{k}}c_{\mathbf{k}+\mathbf{Q}}\ ,\\ \beta_{\mathbf{k}}&=\sin\theta_{\mathbf{k}}c_{\mathbf{k}}+\cos\theta_{\mathbf{k}}c_{\mathbf{k}+\mathbf{Q}}\ ,\end{aligned} \tag{D3}$$

and choose

$$\cos^2\theta_{\mathbf{k}}=\frac{1}{2}\left[1+\frac{\bar{\epsilon}_{\mathbf{k}}}{E_k}\right]$$

and

$$\sin^2\theta_{\mathbf{k}}=\frac{1}{2}\left[1-\frac{\bar{\epsilon}_{\mathbf{k}}}{E_k}\right], \tag{D4}$$

then the Hamiltonian (D1) is diagonal when written in terms of the operators $\alpha_{\mathbf{k}}$ and $\beta_{\mathbf{k}}$. Here we have set $\bar{\mu}=0$ to restrict ourselves to half filling. $E_{\mathbf{k}}=\pm\sqrt{\bar{\epsilon}_{\mathbf{k}}^2+\Delta_c^2}$ are the energy eigenvalues of the new quasiparticles $\alpha_{\mathbf{k}}$ and $\beta_{\mathbf{k}}$. The inverse of the transformation (D3) is

$$\begin{bmatrix}c_{\mathbf{k}}\\ c_{\mathbf{k}+\mathbf{Q}}\end{bmatrix}=\mathcal{S}^{-1}(\theta_k)\begin{bmatrix}\alpha_{\mathbf{k}}\\ \beta_{\mathbf{k}}\end{bmatrix}, \tag{D5}$$

where $\mathcal{S}(\theta_{\mathbf{k}})=\cos\theta_{\mathbf{k}}1-i\sigma_2\sin\theta_{\mathbf{k}}$. Thus in the CDW phase we have two quasiparticle bands with energies $E_{\mathbf{k}}$ and $-E_{\mathbf{k}}$, separated by a gap $2\Delta_c$ along the entire noninteracting Fermi surface.

2. Calculation of the pair susceptibility in the singlet channel

In the extended Hubbard model, the interaction between electrons with antiparallel spin can be written as

$$(-U+2zV\gamma_{\mathbf{k}_1-\mathbf{k}_4})c^{\dagger}_{\mathbf{k}_1\uparrow}c^{\dagger}_{\mathbf{k}_2\downarrow}c_{\mathbf{k}_3\downarrow}c_{\mathbf{k}_4\uparrow}\bar{\delta}_{\mathbf{k}_1+\mathbf{k}_2,\mathbf{k}_3+\mathbf{k}_4}\ , \tag{D6}$$

where the $\bar{\delta}$ function is defined on a lattice and takes care of **umklapp** processes also, i.e., $\mathbf{k}_1+\mathbf{k}_2-\mathbf{k}_3-\mathbf{k}_4$ can be zero or G, a reciprocal-lattice vector. In the CDW state, it is convenient to consider bands with dispersion relations $\bar{\epsilon}_{\mathbf{k}}$ and $\bar{\epsilon}_{\mathbf{k}+\mathbf{Q}}$ as two separate bands labeled 1 and 2. Thus we can decompose the interaction term into various components involving these two bands (Fig. 3). The interaction vertex becomes

$$V_{ij;i'j'}(\mathbf{k},\mathbf{k}')=(-U+s_is_{i'}zV\gamma_{\mathbf{k}-\mathbf{k}'})\theta_{ij;i'j'}\ , \tag{D7}$$

where

$$\theta_{ij;i'j'}=\tfrac{1}{2}(1+s_is_js_{i'}s_{j'}), \tag{D8}$$

i,j, etc., are band indices (1 or 2) and $Sj = l(-1)$, for $j = 1(2)$, The S function in Eq. (D6) now requires that the center-of-mass momentum q of the pair be conserved modulo G (but V does not depend on q).

It is convenient for later purposes to write Eq. (D7) in a separable form. For this we write

$$z\gamma_{\mathbf{k}-\mathbf{k}'}=2\sum_{\mu=1}^{3}\cos(k_\mu-k'_\mu)=2\sum_{\alpha=1}^{6}\phi_\alpha(\mathbf{k})\phi_\alpha(\mathbf{k}')\ , \tag{D9}$$

where

$$\begin{aligned}\phi_\alpha(\mathbf{k})&=\cos k_\alpha,\quad \text{for } 1\le\alpha\le3\ ,\\ \phi_\alpha(\mathbf{k})&=\sin k_{\alpha-3},\quad \text{for } 4\le\alpha\le6\ ,\end{aligned} \tag{D10}$$

and k_1, k_2, and k_3 denote the three Cartesian components of k. We can now write Eq. (D7) as

$$V_{ij;i'j'}(\mathbf{k},\mathbf{k}')=\theta_{ij;i'j'}\sum_{\alpha=0}^{6}v_\alpha\phi_{\alpha,i}(\mathbf{k})\phi_{\alpha,i'}(\mathbf{k}')\ , \tag{D11}$$

where

$$\phi_{\alpha,i}(\mathbf{k})=s_i\phi_\alpha(\mathbf{k})\quad \text{for } 1\le\alpha\le6$$

and

$$\phi_{\alpha,i}(\mathbf{k})=\phi_\alpha(\mathbf{k})=1\quad \text{for } \alpha=0\ ,$$

$$v_\alpha=2V\ \text{ for } 1\le\alpha\le6,\ \ v_\alpha=-U\ \text{ for } \alpha=0\ .$$

In the CDW ground state there are two bands, so there are 16 pair susceptibilities:

$$\chi_{p,ij;i'j'}(\mathrm{q},\nu)=\frac{1}{2\pi N^2}\int_{-\infty}^{+\infty}d\tau\,e^{i\nu\tau}\sum_{\mathbf{k},\mathbf{k}'}{}'\langle T_\tau[c_{\mathbf{k}+\mathbf{q}\uparrow,i'}(\tau)c_{-\mathbf{k}\downarrow,j'}(\tau)c^{\dagger}_{\mathbf{k}'+\mathbf{q}\uparrow,i}(0)c^{\dagger}_{-\mathbf{k}'\downarrow,j}(0)]\rangle\ , \tag{D12}$$

where T_τ represents time-ordering, *i,j,* etc., are band indices, the subscript *p* indicates pairing, and the expectation value is calculated with respect to the interacting ground state. (We restrict ourselves to $T=0$ for the most part, but a finite-temperature generalization is straightforward.)

The Dyson equation for this pair susceptibility in the ladder approximation is described diagrammatically in Fig. 3 and has the form

$$\tilde{\chi}_{ij;i'j'}(k;q)-\sum_{k'}\sum_{l,m,l',m'}\tilde{\chi}^0_{ij;lm}(k;q)V_{lm;l'm'}(\mathbf{k},\mathbf{k}')$$
$$\tilde{\chi}_{l'm';i'j'}(k';q)=\tilde{\chi}^0_{ij;i'j'}(k;q)\,, \qquad \text{(D13)}$$

where $\tilde{\chi}_{ij;i'j'}(k,q)$ is the value of the diagram shown in Fig. 3, with

$$\chi_{p,ij;i'j'}(q)=\sum_k \tilde{\chi}_{ij;i'j'}(k;q)\,, \qquad \text{(D14)}$$

and where we have used the notations $q\equiv(\mathbf{q},\nu)$, fc=(k,ffl), and $\sum_k\equiv(1/N)\sum'_{\mathbf{k}}\int d\omega$. Here $\tilde{\chi}^0(k;q)$ is shown in Fig. 3 and we have

$$\chi^0_{p,ij;i'j'}(q)=\sum_k \tilde{\chi}^0_{ij;i'j'}(k;q)$$
$$=\sum_k G^0_{ii'}(k+q)G^0_{jj'}(-k)\,, \qquad \text{(D15)}$$

where $\chi^0_{p,ij;i'j'}(k;q)$ and $G^0_{ii'}(k)$ are, respectively, the mean-field (two-particle) pair susceptibility and the mean-field, single-particle Green function in the CDW ground state. $G^0_{ii'}(k)$ is the 2×2 matrix (in the basis of $c_{\mathbf{k}\sigma}$)

$$G^{0^{-1}}(\mathbf{k},\omega)=\omega 1-\varepsilon_{\mathbf{k}}\sigma_3+\Delta_c\sigma_1\,. \qquad \text{(D16)}$$

Since the frequency does not appear in the potential, we can rewrite Eq. (D13) in terms of $\tilde{\chi}_{ij;i'j'}(\mathbf{k};q)\equiv\int d\omega\tilde{\chi}_{ij;i'j'}(k;q)$ and a similarly defined $\tilde{\chi}^0_{ij;i'j'}(\mathbf{k};q)$ to get (henceforth we use $\sum_{\mathbf{k}}=(1/N)\sum'_{\mathbf{k}}$)

$$\tilde{\chi}_{ij;i'j'}(\mathbf{k};q)-\sum_{\mathbf{k}'}\sum_{l,m,l',m'}\tilde{\chi}^0_{ij;lm}(\mathbf{k};q)$$
$$\times V_{lm;l'm'}(\mathbf{k},\mathbf{k}')\tilde{\chi}_{l'm';i'j'}(\mathbf{k}';q)=\tilde{\chi}^0_{ij;i'j'}(\mathbf{k};q)\,. \qquad \text{(D17)}$$

Equation (D17) is an integral equation with a separable kernel though this may not be evident at first) and can be solved in a straightforward way. The separability and the solution is simplified greatly if we work in the quasiparticle [$\alpha_{\mathbf{k}}$ and $\beta_{\mathbf{k}}$ of Eq. (D3)] basis rather than the basis of $c_{\mathbf{k}\sigma}$'s since in the quasiparticle basis the mean-field single-particle Green function (D16) is diagonal. In the following we transform Eq. (D17) into the quasiparticle basis and also set q=0. (For the cooperon bound-state energies we need the pair susceptibility at q=0 only.) Some aspects of the $\mathbf{q}\neq0$ case are discussed in Appendix E.

From Eq. (D17) we get, in the quasiparticle basis,

$$\tilde{\chi}_{rs;r's'}(\mathbf{k};\nu)-\sum_{\mathbf{k}'}\sum_{u,v,r'',s''}\tilde{\chi}^0_{rs;uv}(\mathbf{k};\nu)$$
$$\times V_{uv;r''s''}(\mathbf{k},\mathbf{k}')\tilde{\chi}_{r''s'';r's'}(\mathbf{k}';\nu)=\tilde{\chi}^0_{rs;r's'}(\mathbf{k};\nu)\,, \qquad \text{(D18)}$$

where *r,s,u,v,* etc., refer to the quasiparticle bands (and each assumes the values 1 or 2 only).

In the quasiparticle basis the interaction vertex becomes [via Eqs. (D5) and (D11)]:

$$V_{rs;r's'}(\mathbf{k},\mathbf{k}')=\theta_{rs;r's'}(\mathbf{k},\mathbf{k}')\sum_\alpha v_\alpha\phi_{\alpha,r}(\mathbf{k})\phi_{\alpha,r'}(\mathbf{k}')\,, \qquad \text{(D19)}$$

where

$$\phi_{\alpha,r}(\mathbf{k})=\phi_\alpha(\mathbf{k})\xi_r(\mathrm{k}) \quad \text{for } 1\le\alpha\le6\,,$$
$$\phi_{\alpha,i}(\mathbf{k})=\phi_\alpha(\mathbf{k}) \quad \text{for } \alpha=0\,,$$
$$\theta_{rs;r's'}(\mathbf{k},\mathbf{k}')=\tfrac{1}{2}[\xi_r(\mathbf{k})\xi_s(-\mathbf{k})\xi_{r'}(\mathbf{k}')\xi_{s'}(-\mathbf{k}')$$
$$+\xi_r(\mathbf{k})\xi_s(-\mathbf{k})\xi_{r'}(\mathbf{k}')\xi_{s'}(-\mathbf{k}')]\,, \qquad \text{(D20)}$$
$$\xi_r(\mathbf{k})=\sum_j \mathcal{S}_{rj}(\theta_{\mathbf{k}})=\cos\theta_{\mathbf{k}}-s_r\sin\theta_{\mathbf{k}}\,,$$

and (D21)

$$\xi_r(\mathbf{k})=\sum_j \mathcal{S}_{rj}(\theta_{\mathbf{k}})s_j=s_r\cos\theta_{\mathbf{k}}+\sin\theta_{\mathbf{k}}\,.$$

In this basis the mean-field, single-particle Green-function matrix in the CDW state [defined in the basis of $\alpha_{\mathbf{k}}$'s in Eq. (D16)] is diagonal. The elements of this Green-function matrix are

$$\mathcal{G}^{0^{-1}}_{ij}(\mathbf{k},\omega)=\delta_{ij}(\omega-s_iE_{\mathbf{k}})\,, \qquad \text{(D22)}$$

where $E_{\mathbf{k}}$ is the quasiparticle energy defined in Sec. D 1. Now Eq. (D18) can be rewritten as

$$\sum_{\mathbf{k}'}\sum_{u,v;r''s''}[\delta_{\mathbf{kk}'}\delta_{rr''}\delta_{ss''}-\tilde{\chi}^0_{rs;uv}(\mathbf{k};\nu)$$
$$V_{uv;r''s''}(\mathbf{k},\mathbf{k}')]\tilde{\chi}_{r''s'';r's'}(\mathbf{k}';\nu)=\tilde{\chi}^0_{rs;r's'}(k;\nu)\,. \qquad \text{(D23)}$$

The solutions of this integral equation can be obtained in the standard way by using the eigenvalues and eigenfunctions of the kernel. The poles of the pair susceptibility are determined by the zero eigenvalues of this kernel. The eigenvalue equation can be written as

$$[\delta_{rr'}\delta_{ss'}\delta_{\mathbf{kk}'}-\sum_{\mathbf{k}'}\sum_{r's'}\tilde{\chi}^0_r(\mathbf{k};\nu)\delta_{rs}V_{rs;r's'}(\mathbf{k},\mathbf{k}')]$$
$$\times e_{r's'}(\mathbf{k}';\nu)=\lambda e_{rs}(\mathbf{k};\nu)\,, \qquad \text{(D24)}$$

where $e_{rs}(\mathbf{k};\nu)$ is the eigenvector with eigenvalue λ. We have used a simplified form for $\tilde{\chi}^0_{rs;r's'}(\mathbf{k};i\nu_m)$ in the quasiparticle basis which can be easily derived by using Eqs. (D16), (D22),and the definition of $\tilde{\chi}^0_{rs;r's'}(\mathbf{k};q)$ given above. This simplified form for $\tilde{\chi}^0_{rs;r's'}(\mathbf{k};i\nu_m)$ is

$$\tilde{\chi}^0_{rs;r's'}(\mathbf{k};i\nu_m)=\delta_{rr'}\delta_{ss'}\delta_{rs}\frac{1-2f(E_r(\mathbf{k}))}{i\nu_m-2E_r(\mathbf{k})}$$
$$\equiv\delta_{rr'}\delta_{ss'}\delta_{rs}\tilde{\chi}^0_r(\mathbf{k};i\nu_m)\ . \qquad \text{(D25)}$$

We have used the finite-temperature form with $i\nu_m$ the discrete Matsubara frequency, $f(E)$ the Fermi function, and $E_r(\mathbf{k})=\eta_r E_{\mathbf{k}}$, where $\eta_r = 1(-1)$ for r = l (2). Given the form of Eq. (D25), we can choose $e_{rs}(\mathbf{k};\nu)$ to be diagonal in the band indices, i.e., of the form $\delta_{rs}e_r(\mathbf{k};\nu)$. Hence

$$[\delta_{rr'}\delta_{\mathbf{k}\mathbf{k}'}-\sum_{\mathbf{k}'}\sum_{r'}\tilde{\chi}^0_r(\mathbf{k};\nu)V_{rr;r'r'}(\mathbf{k},\mathbf{k}')]e_{r'}(\mathbf{k}';\nu)=\lambda e_r(\mathbf{k};\nu)\ . \qquad \text{(D26)}$$

We give the solution of this equation separately for the cases $V=0$ and $V\neq 0$.

Case I: $V=0$. Let us substitute Eq. (D19) in Eq. (D26) to get

$$e_r(\mathbf{k};\nu)+\frac{U}{2}\sum_{\mathbf{k}'}\sum_{r'}\tilde{\chi}^0_r(\mathbf{k};\nu)[(\xi_r(\mathbf{k})\xi_r(-\mathbf{k})\xi_{r'}(\mathbf{k}')\xi_{r'}(-\mathbf{k}')+\zeta_r(\mathbf{k})\zeta_r(-\mathbf{k})\zeta_{r'}(\mathbf{k}')\zeta_{r'}(-\mathbf{k}')]e_{r'}(\mathbf{k}';\nu)=\lambda e_r(\mathbf{k};\nu)\ . \qquad \text{(D27)}$$

If we multiply both sides of Eq. (D37) by $\xi^2_r(\mathbf{k})$ and sum over r and k we obtain ($\xi_r(\mathbf{k})$ is an even function of k),

$$\sum_{\mathbf{k},r}\xi^2_r(\mathbf{k})e_r(\mathbf{k};\nu)+\frac{U}{2}\sum_{\mathbf{k},\mathbf{k}',r,r'}\tilde{\chi}^0_r(\mathbf{k};\nu)[\xi^4_r(\mathbf{k})\xi^2_{r'}(\mathbf{k}')+\xi^2_r(\mathbf{k})\zeta^2_r(\mathbf{k})\zeta^2_{r'}(\mathbf{k}')]e_{r'}(\mathbf{k};\nu)=\lambda\sum_{\mathbf{k},r}e_r(\mathbf{k};\nu)\xi^2_r(\mathbf{k})\ . \qquad \text{(D28)}$$

Similarly by multiplying both sides of Eq. (D27) by $\zeta^2_r(\mathbf{k})$ and summing over r and k we get [$\zeta_r(\mathbf{k})$ is an even function of k]:

$$\sum_{\mathbf{k},r}\zeta^2_r(\mathbf{k})e_r(\mathbf{k};\nu)+\frac{U}{2}\sum_{\mathbf{k},\mathbf{k}',r,r'}\tilde{\chi}^0_r(\mathbf{k};\nu)[\zeta^2_r(\mathbf{k})\xi^2_r(\mathbf{k})\xi^2_{r'}(\mathbf{k}')+\zeta^4_r(\mathbf{k})\zeta^2_{r'}(\mathbf{k}')]e_{r'}(\mathbf{k}';\nu)=\lambda\sum_{k,r}e_r(\mathbf{k};\nu)\zeta^2_r(\mathbf{k})\ . \qquad \text{(D29)}$$

If we define

$$\sum_{\mathbf{k},r}\xi^2_r(\mathbf{k})e_r(\mathbf{k};\nu)\equiv g_0(\nu)\ ,$$
$$\sum_{\mathbf{k},r}\zeta^2_r(\mathbf{k})e_r(\mathbf{k};\nu)\equiv f_0(\nu)\ ,$$
$$\frac{U}{2}\sum_{\mathbf{k},r}\xi^2_r(\mathbf{k})\zeta^2_r(\mathbf{k})\chi^0_r(\mathbf{k})\equiv R_{00}(\nu)\ ,$$
$$\frac{U}{2}\sum_{\mathbf{k},r}\xi^4_r(\mathbf{k})\tilde{\chi}^0_r(\mathbf{k},r)\equiv\Gamma_{00}(\nu)\ ,$$
$$\frac{U}{2}\sum_{\mathbf{k},r}\zeta^4_r(\mathbf{k})\tilde{\chi}^0_r(\mathbf{k},r)\equiv\Pi_{00}(\nu)\ , \qquad \text{(D30)}$$

we can write Eqs. (D27) and (D28) as a 2X2 matrix eigenvalue problem:

$$\mathcal{M}\begin{bmatrix}/\mathrm{o}\\ g_0\end{bmatrix}\equiv\left[1+\begin{bmatrix}\Gamma_{00} & R_{00}\\ R_{00} & \Pi_{00}\end{bmatrix}\right]\begin{bmatrix}f_0\\ g_0\end{bmatrix}=\lambda\begin{bmatrix}f_0\\ g_0\end{bmatrix}\ . \qquad \text{(D31)}$$

Here we have suppressed the v dependence of the matrix elements for notational convenience. To get the pair susceptibility, we need to solve the equation $\det\mathcal{M}=0$. For the purposes of interest here, this is equivalent to the condition $\lambda_{\max}=0$, where $\lambda_{\max}$ is the largest eigenvalue of M.

Case II: $V\neq 0$. The eigenvalue equation (D26), in the case of $V\neq 0$, is

$$e_r(\mathbf{k};\nu)-\sum_{k'r'}\tilde{\chi}^0_r(\mathbf{k};\nu)\sum_{\alpha=0}^{6}v_\alpha\phi_{\alpha,r}(\mathbf{k})\phi_{\alpha,r'}(\mathbf{k}')e_{r'}(\mathbf{k}';\nu)$$
$$=\lambda e_r(\mathbf{k};\nu)\ . \qquad \text{(D32)}$$

We now define

$$\sum_{\mathbf{k},r}\xi^2_r\phi_{\alpha,r}(\mathbf{k})e_r(\mathbf{k};\nu)\equiv g_\alpha(\nu)\ ,$$
$$\sum_{\mathbf{k},r}\zeta^2_r\phi_{\alpha,r}(\mathbf{k})e_r(\mathbf{k};\nu)\equiv f_\alpha(\nu)\ , \qquad \text{(D33)}$$
$$v_\alpha\sum_{\mathbf{k},r}\chi^0_r(\mathbf{k})\xi^2_r(\mathbf{k})\zeta^2_r(\mathbf{k})\phi_{\alpha,r}(\mathbf{k})\phi_{\beta,r}(\mathbf{k})\equiv R_{\beta\alpha}(\nu)\ .$$

Next we multiply Eq. (D32) by $\xi^2_r(\mathbf{k})\phi_{\beta,r}(\mathbf{k})$ on both sides and sum over k and r to get

$$g_\beta-\sum_\alpha\Gamma_{\beta\alpha}g_\alpha-\sum_\alpha R_{\beta\alpha}f_\alpha=\lambda g_\beta\ - \qquad \text{(D34)}$$

Similarly if we multiply Eq. (D32) by $\zeta^2_r(\mathbf{k})\phi_{\beta,r}(\mathbf{k})$ on both sides and sum over k and r we get

$$f_\beta-\sum_\alpha\Pi_{\beta\alpha}f_\alpha-\sum_\alpha R_{\beta\alpha}g_\alpha=\lambda f_\beta\ , \qquad \text{(D35)}$$

where

$$\Gamma_{\beta\alpha}(\nu)\equiv v_\alpha\sum_{\mathbf{k},r}\phi_{\beta,r}(\mathbf{k})\phi_{\alpha,r}(\mathbf{k})\chi^0_r(\mathbf{k};\nu)\xi^4_r(\mathbf{k})\ ,$$
$$\Pi_{\beta\alpha}(\nu)\equiv v_\alpha\sum_{\mathbf{k},r}\phi_{\beta,r}(\mathbf{k})\phi_{\alpha,r}(\mathbf{k})\chi^0_r(\mathbf{k};\nu)\zeta^4_r(\mathbf{k})\ . \qquad \text{(D36)}$$

Equations (D34) and (D35) can be written as matrix equations:

$$\sum_\alpha[(\delta_{\alpha\beta}-\Gamma_{\beta\alpha})g_\alpha-R_{\beta\alpha}f_\alpha]=\lambda g_\beta$$

and

$$\sum_\alpha[(\delta_{\alpha\beta}-\Pi_{\beta\alpha})f_\alpha-R_{\beta\alpha}g_\alpha]=\lambda f_\beta\ . \qquad \text{(D37)}$$

The set of equations (D37) is a 14X 14 matrix equation of the form

$$\mathcal{M}_p \begin{bmatrix} f_\alpha \\ g_\beta \end{bmatrix} \equiv (1-\mathcal{R}) \begin{bmatrix} f_\alpha \\ 80 \end{bmatrix} = \lambda \begin{bmatrix} f_\alpha \\ g_\beta \end{bmatrix}, \tag{D38}$$

where 1 denotes a 14X 14 unit matrix. The poles of the pair-susceptibility $\chi_p(\mathbf{q}=0,\nu)$ are obtained from the condition that the determinant of the matrix $\mathcal{M}_p$ vanishes.

Let us show a few matrix elements explicitly. At zero temperature the expressions for the pair susceptibilities [Eq. (D21)] yield via standard analytic continuation onto the real v axis ($i\nu_m \rightarrow \nu + i\eta$),

$$\tilde{\chi}_1^0(\mathbf{k};\nu) = \frac{1}{\nu - 2E_{\mathbf{k}}} \quad \text{and} \quad \tilde{\chi}_2^0(\mathbf{k};\nu) = -\frac{1}{\nu + 2E_{\mathbf{k}}}. \tag{D39}$$

If we define

$$\Omega_1(\mathbf{k};\nu) \equiv \sum_r \xi_r^4(\mathbf{k}) \xi_r^2(\mathbf{k}) \tilde{\chi}_r^0(\mathbf{k};\nu) = \left[\frac{(1-\Delta_c/E_{\mathbf{k}})}{\nu - 2E_{\mathbf{k}}} - \frac{(1+\Delta_c/E_{\mathbf{k}})}{\nu + 2E_{\mathbf{k}}} \right] \frac{\tilde{\epsilon}_{\mathbf{k}}^2}{E_{\mathbf{k}}^2},$$

$$\Omega_2(\mathbf{k};\nu) \equiv \sum_r \xi_r^6(\mathbf{k}) \chi_r^0(\mathbf{k},r),$$

and

$$\Omega_3(\mathbf{k};\nu) \equiv \sum_r \xi_r^4(\mathbf{k}) \xi_r^2(\mathbf{k}) \chi_r^0(\mathbf{k};\nu) = \Omega_1(\mathbf{k};-\nu), \tag{D40}$$

then the following matrix elements can be written as

$$\Gamma_{12} = V \sum_{\mathbf{k}} \Omega_1(\mathbf{k};\nu) \cos k_x \cos k_y,$$

$$\Pi_{22} = V \sum_{\mathbf{k}} \Omega_2(\mathbf{k};\nu) \cos^2 k_y,$$

$$R_{32} = V \sum_{\mathbf{k}} \Omega_3(\mathbf{k};\nu) \cos k_z \cos k_y,$$

$$R_{42} = V \sum_{\mathbf{k}} \Omega_3(\mathbf{k};\nu) \sin k_x \cos k_y,$$

etc. From this it is not hard to see that $\mathcal{M}_p$ and $\mathcal{R}$ have block-diagonal structures, since any sum of the form $\sum'_{k_x} \sin k_x f(k)$, where $f(k_x)$ is an even function, is zero by parity. Thus the matrices $\mathcal{M}_p$ and $\mathcal{R}$ are both block diagonal with one 8×8 and one 6×6 block each.

The top 8 X 8 block of the matrix $\mathcal{R}$ is

$$\begin{bmatrix}
\Gamma_{00} & R_{00} & \Gamma_{01} & R_{01} & \Gamma_{02} & R_{02} & \Gamma_{03} & R_{03} \\
R_{00} & \Pi_{00} & R_{01} & \Pi_{01} & R_{02} & \Pi_{02} & R_{03} & \Pi_{03} \\
\Gamma_{10} & R_{10} & \Gamma_{11} & R_{11} & \Gamma_{12} & R_{12} & \Gamma_{13} & R_{13} \\
R_{10} & \Pi_{10} & R_{11} & \Pi_{11} & R_{12} & \Pi_{12} & R_{13} & \Pi_{13} \\
\Gamma_{20} & R_{20} & \Gamma_{21} & R_{21} & \Gamma_{22} & R_{22} & \Gamma_{23} & R_{23} \\
R_{20} & \Pi_{20} & R_{21} & \Pi_{21} & R_{22} & \Pi_{22} & R_{23} & \Pi_{23} \\
\Gamma_{30} & R_{30} & \Gamma_{31} & R_{31} & \Gamma_{32} & R_{32} & \Gamma_{33} & R_{33} \\
R_{30} & \Pi_{30} & R_{31} & \Pi_{31} & R_{32} & \Pi_{32} & R_{33} & \Pi_{33}
\end{bmatrix}. \tag{D41}$$

Note the following points.

(a) The upper left 2×2 block is the matrix obtained in the $V=0$ case discussed earlier.

(b) The elements in the first two columns of this matrix depend on U and are independent of V. All the rest of the elements depend on V and do not depend on U.

(c) The lower 6X6 block, obtained from the above 8×8 block by considering elements other than the first two rows and columns, is a symmetric block.

(d) The largest eigenvalue of the full matrix $\mathcal{M}_p$ can be obtained by diagonalizing the above 8X8 block. We require the determinant of $\mathcal{M}_p$ to vanish to obtain the poles of $\chi_p(\mathbf{q}=\mathbf{0},\nu)$; this is equivalent to the vanishing of the determinant of the upper 8×8 block. The value of the frequency v at which this determinant vanishes gives the pole of the pair susceptibility.

APPENDIX E: PSEUDOSPIN-WAVE EXCITATION IN THE NEGATIVE-U HUBBARD MODEL

In this appendix we discuss some aspects of $\chi_p(\mathbf{q},\nu)$ for $\mathbf{q}\neq0$. We do this only for $V=0$, as the calculations with $V\neq0$ are numerically very complicated. The essential results of the pseudospin-wave theory (valid at large U) can be demonstrated in the $V=0$ case quite neatly. The main result we obtain is that the excitation spectrum for the negative-U Hubbard model, derived from the poles of the pair susceptibility in the CDW state at any U, reproduces the excitation spectrum of the large-U limit of this model (obtainable from the pseudospin Heisenberg model,[2] $H_{\text{spin}} = J/2 \sum_{\langle ij \rangle} (\mathbf{S}_i \cdot \mathbf{S}_j - \frac{1}{4})$, where $J = 4\tilde{t}^2/U$). We also show that the excitation spectrum obtained in the ladder approximation for the CDW state of the negative-U Hubbard model is identical to the corresponding RPA excitation spectrum[29,30] of the positive-U Hubbard model in its spin-density-wave phase (for the equivalence of these two models at half filling see Sec. II).

To obtain the excitation spectrum in the case where $\mathbf{q}\neq0$ and $V=0$, we require the poles of the pair susceptibility at $V=0$, i.e., the determinant of the following 2×2 matrix $\mathcal{M}_p$ should vanish:

$$\mathcal{M}_p = 1 + \begin{bmatrix} \Gamma_{00}(\mathbf{q},\nu) & R_{00}(\mathbf{q},\nu) \\ R_{00}(\mathbf{q},\nu) & \Pi_{00}(\mathbf{q},\nu) \end{bmatrix} \equiv 1 + \frac{U}{2} \begin{bmatrix} \chi_{11}^0(\mathbf{q},\nu) & \chi_{12}^0(\mathbf{q},\nu) \\ \chi_{21}^0(\mathbf{q},\nu) & \chi_{22}^0(\mathbf{q},\nu) \end{bmatrix}, \tag{E1}$$

where

$$\chi_{11}^0(\mathbf{q},\nu) \equiv \frac{2}{U} \Gamma_{00}(\mathbf{q},\nu) = \sum_{\mathbf{k}} \left[\frac{(1-\Delta_c/E_{\mathbf{k}})(1-\Delta_c/E_{\mathbf{k}+\mathbf{q}})}{\nu - E_{\mathbf{k}} - E_{\mathbf{k}+\mathbf{q}}} - \frac{(1+\Delta_c/E_{\mathbf{k}})(1+\Delta_c/E_{\mathbf{k}+\mathbf{q}})}{\nu + E_{\mathbf{k}} + E_{\mathbf{k}+\mathbf{q}}} \right],$$

$$\frac{U}{2} \chi_{22}^0(\mathbf{q},\nu) \equiv \Pi_{00}(\mathbf{q},\nu) = \Gamma_{00}(\mathbf{q},-\nu) \equiv \frac{U}{2} \chi_{11}^0(\mathbf{q},-\nu), \tag{E2}$$

and

$$\chi^0_{12}(\mathbf{q},\nu)=\chi^0_{21}(\mathbf{q},\nu)=\frac{2}{U}R_{00}(\mathbf{q},\nu)$$

$$=2\sum_{\mathbf{k}}\frac{\tilde{\epsilon}_{\mathbf{k}}\tilde{\epsilon}_{\mathbf{k}+\mathbf{q}}}{E_{\mathbf{k}}E_{\mathbf{k}+\mathbf{q}}}\frac{E_{\mathbf{k}}+E_{\mathbf{k}+\mathbf{q}}}{\nu^2-(E_{\mathbf{k}}+E_{\mathbf{k}+\mathbf{q}})^2}\ ,$$

where all symbols have been defined in Appendix D or earlier.

The mean-field pair susceptibility in the CDW phase is the 2×2 matrix

$$\Xi^0_p=\begin{bmatrix}\chi^0_{11}(\mathbf{q},\nu) & \chi^0_{12}(\mathbf{q},\nu)\\ \chi^0_{21}(\mathbf{q},\nu) & \chi^0_{22}(\mathbf{q},\nu)\end{bmatrix},$$

which obeys the symmetry property $\Xi^0_p(\mathbf{q}+\mathrm{Q},\nu)=\sigma_3\Xi^0_p(\mathbf{q},\nu)\sigma_3$, where σ_3 is the third **Pauli** matrix and Q is the zone-corner wave vector $\pi/a(1,1,1)$. The pair susceptibility matrix in the CDW state in the F=0 case is given by $\Xi^0_p\mathcal{M}_p^{-1}$, where $\mathcal{M}_p^{-1}$ is the inverse of $\mathcal{M}_p$ defined above.

The negative-U Hubbard model has a pseudospin rotation symmetry at half filling (Sec. II). In the CDW state this symmetry is spontaneously broken. Hence there will be Goldstone modes in this phase. In the large, **negative-U** limit, i.e., for the pseudospin model, these gapless modes are the transverse, pseudospin-wave excitations in the antiferromagnetic phase, which breaks the pseudospin-rotation symmetry of the Heisenberg model.

The bound-state energy of the two-particle excitation spectrum at half filling in the CDW state at q=0 goes to zero as $V\to0$ (Sec. II), i.e., the pseudospin-rotation symmetry (broken by the F term) of the Hubbard Hamiltonian is restored, the spectrum becomes gapless. Hence the energy of this bound state as a function of momentum (for small momentum) yields the spectrum of the low-lying modes. As this state is at zero energy for q=0, we can make an expansion in the energy and momentum close to zero to get the spectrum of the lowest-lying modes at small q and frequency ν. At large U we find that the spectrum evolves smoothly into the pseudospin-wave spectrum of the Heisenberg model. This shows clearly that there is a smooth interpolation of the zero-temperature excitation spectra, at least at the level of **RPA** calculations. We give the details of our calculation here, which is similar to that of Singh and Tesanović.[30]

The condition $\det\mathcal{M}_p=0$ turns out to be equivalent to

$$\lambda_{\max}+1/U=0\ , \tag{E3}$$

where $\lambda_{\max}$ is the largest eigenvalue of $\frac{1}{2}\Xi^0_p(\mathbf{q},\nu)$. We do a **small-$\nu$** and **small-q** expansion to get the spectrum. Note that the minimum value of $E_{\mathbf{k}}+E_{\mathbf{k}+\mathbf{q}}$ is $2\Delta_c$ which, in the $U\to\infty$ limit, is just U. Hence, for $\nu\to0$, $\nu/2\Delta_c$ is the expansion parameter we use.

The **off-diagonal** terms of Ξ^0_p, $\chi^0_{12}(\mathbf{q},\nu)$, **and** $\chi^0_{21}(\mathbf{q},\nu)$, do not contain any term linear in ν, so the leading term in their expansion above v=0 is $O(\nu^2)$. If we write

$$\tfrac{1}{2}\chi^0_{11}(\mathbf{q},\nu)=c_2(\mathbf{q},\nu)+\nu c_1(\mathbf{q})\ ,$$

$$\tfrac{1}{2}\chi^0_{22}(\mathbf{q},\nu)=c_2(\mathbf{q},\nu)-\nu c_1(\mathbf{q})\ ,$$

where $c_2(\mathbf{q},\nu)$ contains terms of order higher than v, whereas $c_1(\mathbf{q})$ is independent of v, then

$$\lambda_{\max}=c_2(\mathbf{q},\nu)+\frac{1}{2}|\chi^0_{12}(\mathbf{q},\nu)|+\frac{c_1^2(\mathbf{q})\nu^2}{|\chi^0_{12}(\mathbf{q},\nu)|}\ , \tag{E4}$$

where we have used $\chi^0_{12}(\mathbf{q},\nu)=\chi^0_{21}(\mathbf{q},\nu)$. Since the leading v dependence of the off-diagonal terms $\chi^0_{12}(\mathbf{q},\nu)$ **and** $\chi^0_{21}(\mathbf{q},\nu)$ is $O(\nu^2)$, the leading v-dependent term in the expansion of $\lambda_{\max}$ is $O(\nu^2)$. One can similarly argue that the leading q-dependent term in $\lambda_{\max}$ is of $O(q^2)$. This can be verified by a direct expansion to this order

$$\lambda_{\max}\approx-\frac{1}{U}+\left[h_0+\frac{c_{20}^2}{2s_0}\right]\nu^2-\bar{\omega}(q_1,q_2,q_3)\ , \tag{E5}$$

where h_0, s_0, and c_{20} are constants independent of ν and q, and 55 depends quadratically on the Cartesian components of q denoted by q_α, where $\alpha=1\cdots3$. One has

$$s_0=-\frac{1}{2U}+\frac{\Delta_c^2}{2}\sum_{\mathbf{k}}\frac{1}{E_{\mathbf{k}}^3}\ ,$$

$$c_{20}=-\frac{\Delta_c}{2}\sum_{\mathbf{k}}\frac{1}{E_{\mathbf{k}}^3}\ , \tag{E6}$$

$$h_0=-\frac{1}{4}\sum_{\mathbf{k}}\frac{1}{E_{\mathbf{k}}^3}\ ;$$

and, by using the symmetry of the cubic lattice,

$$\bar{\omega}=\frac{3}{2}\sum_{\mathbf{k}}\frac{\tilde{\epsilon}_{\mathbf{k}}^2}{E_{\mathbf{k}}^5}(2\tilde{t}\sum_\alpha q_\alpha\sin k_\alpha)^2-\sum_{\mathbf{k}}\frac{(2\tilde{t}\sum_\alpha q_\alpha\sin k_\alpha)^2}{E_{\mathbf{k}}^3}$$

$$-\frac{1}{2}\sum_{\mathbf{k}}\frac{\tilde{\epsilon}_{\mathbf{k}}}{E_{\mathbf{k}}^3}(2\tilde{t}\sum_\alpha q_\alpha^2\cos k_\alpha)\ ,$$

which together with $\tilde{\epsilon}_{\mathbf{k}}=2\tilde{t}\sum_\alpha\cos k_\alpha$ yields

$$\bar{\omega}=q^2\tilde{t}^2\sum_{\mathbf{k}}\frac{\sin^2k_x(1-3\tilde{\epsilon}_{\mathbf{k}}^2)/2E_{\mathbf{k}}^2-\frac{1}{2}\cos^2k_x-\cos k_y\cos k_z}{E_{\mathbf{k}}^3}\ . \tag{E7}$$

By substituting Eqs. (E5)-(E7) in Eq. (E3) we get the excitation spectrum in the **CDW** phase: $\nu(\mathbf{q})=v_sq$, where

$$v_s=\left[\frac{2s_0w}{2s_0h_0+c_{20}^2}\right]^{1/2}\ , \tag{E8}$$

and w is the coefficient of q^2 in Eq. (E7).

The **large-U** limit of Eq. (E8) yields the **spin-wave** velocity of the Heisenberg model that obtains in this limit. In the **large-U** limit $E_{\mathbf{k}}\to\Delta_c$. For any dimension d, by keeping terms of order Δ_c^{-3}, we get the spin-wave spec-

trum $\nu(\mathbf{q})=(J/2)z\sqrt{1-\gamma_q^2}$, where $\gamma_{\mathbf{q}}=(1/z)\sum_{\mathbf{a}}e^{i\mathbf{q}\cdot\mathbf{a}}$. In the $\mathbf{q}\to 0$ limit $\gamma_{\mathbf{q}}^2\to 1-q^2/d$, so $\nu(\mathbf{q})=(J/2)zq/\sqrt{d}$. As $z=2d$ for a hypercubic lattice.

$$\nu(\mathbf{q})=\sqrt{d}\,Jq\ , \tag{E9}$$

as expected for the Heisenberg antiferromagnet in linear spin-wave theory. The same result was obtained by Schrieffer, Wen, and Zhang,[29] and by Singh and Tesanović.[30] Our calculation of $\Xi_p^0(\mathbf{q},\nu)$ is more general, though.

APPENDIX F: A COMPARISON OF THE OPTICAL CONDUCTIVITIES IN THE ONE- AND TWO-PARTICLE CHANNELS

For the purposes of illustration we work in the large-U limit of the negative-U, extended Hubbard model and show that the conductivity in the one-particle channel is nearly a factor of 10 smaller than in the two-particle channel. We begin with the two-particle channel, so the charge carriers are cooperons (in the CDW phase we consider), for which we write an effective boson model whose conductivity we calculate.

The anisotropic Heisenberg model that is obtained in the large-U limit of the negative-U, extended-Hubbard model can be written as

$$H=\frac{1}{2}\sum_{\langle ij\rangle}\left[\frac{J_\perp}{2}(\tilde{s}_i^+\tilde{s}_j^+ +\text{H.c.})-J_z\tilde{s}_i^z\tilde{s}_j^z\right]\ , \tag{F1}$$

by using the transformations $s_i^\pm\to\tilde{s}_i^\mp$ and $s_i^z\to-\tilde{s}_i^z$ on one sublattice only, where $s_i^\pm$, are conventional spin operators.[2] [Note that this makes the mean-field ground state of model (F1) ferromagnetic, i.e., $\langle\tilde{s}_i^z\rangle=\frac{1}{2}$, for all i.] From this Hamiltonian it is easy to see[2] that the current operator is

$$\mathbf{j}=-ie\sum_{\langle ij\rangle}J_\perp\mathbf{a}(\tilde{s}_i^+\tilde{s}_j^+ -\text{H.c.})e^{i\mathbf{Q}\cdot\mathbf{r}_i}\ . \tag{F2}$$

We now make the linear spin-wave approximation $\tilde{s}_i^-\to a_i$ and $\tilde{s}_i^z\to(a_i^\dagger a_i-1/2)$, where a_i, etc., are boson operators, and rewrite Eq. (F1) as

$$\mathcal{H}=-\frac{J_z}{4}\frac{Nz}{2}+\frac{1}{4}\begin{pmatrix}a_{\mathbf{k}}^\dagger & a_{-\mathbf{k}}\end{pmatrix}\begin{bmatrix}J_z & J_\perp\gamma_{\mathbf{k}}\\ J_\perp\gamma_{\mathbf{k}} & J_z\end{bmatrix}\begin{pmatrix}a_{\mathbf{k}}\\ a_{-k}^\dagger\end{pmatrix}\ , \tag{F3}$$

where we have Fourier transformed the resulting Hamiltonian and $\gamma_{\mathbf{k}}$ is defined in Appendix A. This Hamiltonian is diagonalized by the usual transformation to the quasiparticle operators $\alpha_{1\mathbf{k}}$ and $\alpha_{2\mathbf{k}}$:

$$\begin{pmatrix}a_{-\mathbf{k}}^\dagger\\ a_{\mathbf{k}}\end{pmatrix}=\begin{bmatrix}-S_{\mathbf{k}} & -C_{\mathbf{k}}\\ C_{\mathbf{k}} & S_{\mathbf{k}}\end{bmatrix}\begin{pmatrix}\alpha_{1\mathbf{k}}\\ \alpha_{2\mathbf{k}}^\dagger\end{pmatrix}\ , \tag{F4}$$

where

$$C_{\mathbf{k}}^2=\frac{1}{2}\left[\frac{J_z}{\sqrt{J_z^2-J_\perp^2\gamma_{\mathbf{k}}^2}}+1\right]$$

and

$$S_{\mathbf{k}}^2=\frac{1}{2}\left[\frac{J_z}{\sqrt{J_z^2-J_\perp^2\gamma_{\mathbf{k}}^2}}-1\right]\ .$$

In the quasiparticle basis the Hamiltonian (F3) becomes

$$\mathcal{H}=\frac{J_z}{4}\frac{Nz}{2}+\sum_{\mathbf{k}}v_{\mathbf{k}}(\alpha_{1\mathbf{k}}^\dagger\alpha_{1\mathbf{k}}+\alpha_{2\mathbf{k}}^\dagger\alpha_{2\mathbf{k}}+1)\ , \tag{F5}$$

where $v_{\mathbf{k}}=J_z^2-J_\perp^2\gamma_{\mathbf{k}}^2$.

The Green functions for the original Hamiltonian (F3) can be written as

$$\begin{bmatrix}\langle\langle a_{\mathbf{k}};a_{\mathbf{k}}^\dagger\rangle\rangle_\omega & \langle\langle a_{\mathbf{k}}^\dagger;a_{-\mathbf{k}}\rangle\rangle_\omega\\ \langle\langle a_{-\mathbf{k}}^\dagger;a_{\mathbf{k}}\rangle\rangle_\omega & \langle\langle a_{-\mathbf{k}};a_{-\mathbf{k}}^\dagger\rangle\rangle_\omega\end{bmatrix}$$
$$=\frac{1}{\omega-v_{\mathbf{k}}}\begin{bmatrix}C_{\mathbf{k}}^2 & -S_{\mathbf{k}}C_{\mathbf{k}}\\ -S_{\mathbf{k}}C_{\mathbf{k}} & S_{\mathbf{k}}^2\end{bmatrix}-\frac{1}{\omega+v_{\mathbf{k}}}\begin{bmatrix}S_{\mathbf{k}}^2 & -S_{\mathbf{k}}C_{\mathbf{k}}\\ -S_{\mathbf{k}}C_{\mathbf{k}} & C_{\mathbf{k}}^2\end{bmatrix}\ , \tag{F6}$$

where the double angular brackets are used following Zubarev[39] to denote Green functions. The conductivity is related to the imaginary part of the current-current correlation function via

$$\sigma_{\mu\nu}(\omega)=\frac{1}{\omega}\mathcal{G}\langle\langle\mathbf{j}_\mu;\mathbf{j}_\nu\rangle\rangle\ . \tag{F7}$$

We can rewrite the current operator (F2) as

$$\mathbf{j}=ezJ_\perp\sum_{\mathbf{k}}\frac{\partial\gamma_{\mathbf{k}}}{\partial\mathbf{k}}(a_{\mathbf{k}}^\dagger a_{\mathbf{Q}-\mathbf{k}}^\dagger+\text{H.c.})\ ,$$

so

$$\langle\langle\mathbf{j}_\alpha;\mathbf{j}_\beta\rangle\rangle=(ezJ_\perp)^2\sum_{\mathbf{k},\mathbf{k}'}\frac{\partial\gamma_{\mathbf{k}}}{\partial\mathbf{k}_\alpha}\frac{\partial\gamma_{\mathbf{k}'}}{\partial k'_\beta}\times\langle\langle(a_{\mathbf{k}}^\dagger a_{\mathbf{Q}-\mathbf{k}}^\dagger+\text{H.c.});(a_{\mathbf{k}'}^\dagger a_{\mathbf{Q}-\mathbf{k}'}^\dagger+\text{H.c.})\rangle\rangle\ . \tag{F8}$$

A Wick decoupling of the right-hand side of Eq. (F8) into products of two-point correlation function yields

$$\langle\langle\mathbf{j}_\alpha;\mathbf{j}_\beta\rangle\rangle=2(ezJ_\perp)^2\times\sum_{\mathbf{k}}\frac{\partial\gamma_{\mathbf{k}}}{\partial k_\alpha}\frac{\partial\gamma_{\mathbf{k}}}{\partial k_\beta}[2n(v_{\mathbf{k}})+1]\times\left[\frac{1}{\omega-2v_{\mathbf{k}}}-\frac{1}{\omega+2v_{\mathbf{k}}}\right]\ , \tag{F9}$$

which along with Eq. (F7) gives

$$\sigma(\omega)=2(ezJ_\perp)^2\sum_{\mathbf{k}}\frac{\partial\gamma_{\mathbf{k}}}{\partial k_\alpha}\frac{\partial\gamma_{\mathbf{k}}}{\partial k_\beta}\frac{[2n(v_{\mathbf{k}})+1]}{2v_{\mathbf{k}}}\delta(\omega-2v_{\mathbf{k}})\ , \tag{F10}$$

where $2n(v_{\mathbf{k}})$ is the Bose distribution function. Hence the zero-temperature conductivity is given by

$$\sigma(\omega)=2(ezJ_\perp)^2\sum_{\mathbf{k}}\frac{\partial\gamma_{\mathbf{k}}}{\partial k_\alpha}\frac{\partial\gamma_{\mathbf{k}}}{\partial k_\beta}\frac{\delta(\omega-2v_{\mathbf{k}})}{2v_{\mathbf{k}}}\ . \tag{F11}$$

The conductivity in the single-particle channel

In the mean-field, CDW phase, the Hamiltonian can be written as

$$\mathcal{H}=\sum_{\mathbf{k}\sigma}{}'(c^\dagger_{\mathbf{k}\sigma}\quad c^\dagger_{\mathbf{k}+\mathbf{Q}\sigma})\begin{pmatrix}\epsilon_{\mathbf{k}} & \mathrm{A}\\ \mathrm{A} & -\epsilon_{\mathbf{k}}\end{pmatrix}(c_{\mathbf{k}\sigma}\quad c_{\mathbf{k}+\mathbf{Q}\sigma})$$
$$=\sum_{\mathbf{k}\sigma}{}'\psi^\dagger_{\mathbf{k}\sigma}M_{\mathbf{k}}\psi_{\mathbf{k}\sigma}\ , \tag{F12}$$

which defines the two-component spinor ψ and the 2×2 matrix M. The prime over the summation indicates that we restrict ourselves to half the Brillouin zone. The current operator for the Hamiltonian (F12) is

$$\mathbf{j}=-ezt\sum_{\mathbf{k}\sigma}{}'\frac{\partial\gamma_{\mathbf{k}}}{\partial\mathbf{k}}\psi^\dagger_{\mathbf{k}\sigma}\tau_3\psi_{\mathbf{k}\sigma}\ , \tag{F13}$$

where τ_3 is the third Pauli matrix and t is the hopping matrix element for the electrons.

For the one-particle channel also we use the RPA to get

$$\langle\langle j_\alpha;j_\beta\rangle\rangle=-2(ezt)^2\sum_{\nu,k}{}'\frac{\partial\gamma_{\mathbf{k}}}{\partial' a}\frac{\partial\gamma_{\mathbf{k}}}{\partial k_\beta}\mathrm{tr}\{\tau_3(\nu\mathbf{1}-M_{\mathbf{k}})^{-1}\tau_3[(\nu+\omega)\mathbf{1}-M_{\mathbf{k}}]^{-1}\}\ . \tag{F14}$$

The right-hand side of Eq. (F14) can be simplified by noting that

$$\mathrm{tr}\{\tau_3(\nu\mathbf{1}-M_{\mathbf{k}})^{-1}\tau_3[(\nu+\omega)\mathbf{1}-M_{\mathbf{k}}]^{-1}\}=\frac{\mathrm{tr}[\nu\tau_3+\epsilon_{\mathbf{k}}+i\Delta\tau_2][(\nu+\omega)\tau_3+\epsilon_{\mathbf{k}}+i\Delta\tau_2]}{(\nu^2-E^2_{\mathbf{k}})[(\omega+\nu)^2-E^2_{\mathbf{k}}]}\ , \tag{F15}$$

where $E^2_{\mathbf{k}}=\Delta^2+\epsilon^2_{\mathbf{k}}$ is the quasiparticle energy in the CDW state, the trace is easily performed to get

$$2\frac{\nu(\nu+\omega)+\epsilon^2_{\mathbf{k}}-\Delta^2}{(\nu^2-E^2_{\mathbf{k}})[(\omega+\nu)^2-E^2_{\mathbf{k}}]}\ ,$$

and the straightforward summation over ν yields

$$\langle\langle j_\alpha;j_\beta\rangle\rangle=2(ezt)^2\sum_{\mathbf{k}}\frac{\partial\gamma_{\mathbf{k}}}{\partial k_\alpha}\frac{\partial\gamma_{\mathbf{k}}}{\partial k_\beta}\left[\frac{\Delta}{E_{\mathbf{k}}}\right]^2[1-2f(E_{\mathbf{k}})]\left[\frac{1}{\omega-2E_{\mathbf{k}}}-\frac{1}{\omega+2E_{\mathbf{k}}}\right]\ . \tag{F16}$$

At zero temperature the conductivity becomes

$$\sigma_{\alpha\beta}(\omega)=2(ezt)^2\sum_{\mathbf{k}}\frac{\partial\gamma_{\mathbf{k}}}{\partial k_\alpha}\frac{\partial\gamma_{\mathbf{k}}}{\partial k_\beta}\left[\frac{\Delta}{E_{\mathbf{k}}}\right]^2\frac{\delta(\omega-2E_{\mathbf{k}})}{E_{\mathbf{k}}}\ . \tag{F17}$$

An estimate of the ratio of the conductivities can be made with the realistic values of different parameters as given in the text; such an estimate shows that the conductivity in the one-particle channel is about a factor of 10 smaller than in the two-particle channel (Fig. 6).

*Present address: Laboratoire d'études des Proprietés Electroniques des Solides, Centre National de la Recherche Scientifique, B. P. 166, 38042, Grenoble, France.

†Also at J. N. Centre for Advanced Scientific Research, Bangalore 560012, India.

[1]A. W. Sleight, J. L. Gillson, and P. E. Bierstedt, Solid State Commun. 17, 27 (1975); A. W. Sleight, in *Chemistry of Oxide Superconductors*, edited by C. N. R. Rao (Blackwell Scientific, Oxford, 1988), p. 27.

[2]For an up-to-date review of the experimental phenomenology and theoretical modeling of barium bismuthates, see, A. Taraphder, H. R. Krishnamurthy, R. Pandit, and T. V. Ramakrishnan (unpublished); A. Taraphder, Ph.D. thesis, Indian Institute of Science, 1991.

[3]T. M. Rice and L. Sneddon, Phys. Rev. Lett. 47, 689 (1981); E. Jurczek and T. M. Rice, Europhys. Lett. 1, 225 (1986); E. Jurczek, Phys. Rev. B 32, 4708 (1985).

[4]C. M. Varma, Phys. Rev. Lett. 61, 2713 (1989).

[5]A. Taraphder, H. R. Krishnamurthy, R. Pandit, and T. V. Ramakrishnan, Europhys. Lett. 21, 79 (1993).

[6]For a review of $BaPb_{1-x}Bi_xO_3$ see S. Uchida, K. Kitazawa, and S. Tanaka, Phase Transitions 8, 95 (1987).

[7]L. F. Matthesis, E. M. Gyorgy, and D. W. Jonston, Jr., Phys. Rev. B 37, 3745 (1988); R. J. Cava, B. Batlogg, J. J. Krajewski, R. Farrow, L. W. Rupp, Jr., A. E. White, K. Short, W. F. Peck, and T. Kometani, Nature (London) 332, 814 (1988).

[8]Many of the actual structures encountered are monoclinic, orthorhombic or rhombohedral, involving (monoclinic) expansions, contractions and rigid rotations of the oxygen octahedra.

[9]R. J. Cava and B. Batlogg, Mater. Res. Bull. 49, Suppl. 4, 309 (1989); B. Batlogg, R. J. Cava, L. F. Schneemeyer, and G. P. Espinosa, IBM J. Res. Dev. 33, 208 (1989).

[10]S. Pei, N. J. Zalusec, J. D. Jonston, D. G. Hinks, A. W. Mitchell, and D. R. Richards, Phys. Rev. B 39, 811 (1989); S.

Pei *et al.*, *ibid.* *41*, 4126 (1990).
[11]C. K. Loong *et al.*, Phys. Rev. Lett. 66, 3217 (1991); Wei Jin *et al.*, Phys. Rev. B 45, 8045 (1992); Q. Huang *et al*, Nature (London) 347, 369 (1992); D. Nguyen *et al*, Solid State Commun. 79, 723 (1991); D. G. Hinks *et al.*, Nature (London) 335, 419 (1988).
[12]Y. J. Uemura *et al.*, Nature (London) 335, 151 (1988); B. Batlogg *et al.*, Phys. Rev. Lett. 61, 1670 (1988); R. J. Cava *et al*, Nature (London) 339, L291 (1989).
[13]N. Jones, J. Parise, R. Flippen, and A. W. Sleight, J. Solid State Chem. Lett. 38, 319 (1989); D. G. Hinks, B. Dabrowski, J. D. Jorgensen, A. W. Mitchell, D. R. Richards, S. Pei, and Donglu Shi, Nature (London) 333, 836 (1988); R. Seshadri, V. Manivannan, K. P. Rajeev, J. Gopalakrishnan, and C. N. R. Rao, J. Solid State Chem. Lett. 89, 389 (1990).
[14]L. F. Matthesis and D. R. Hamman, Phys. Rev. B 28, 4227 (1983); 26, 2686 (1982); Phys. Rev. Lett. 60, 2681 (1988).
[15]S. Sugai *et al.*, Phys. Rev. Lett. 55, 426 (1985); Jpn. J. Appl. Phys. 24, Suppl. 24-2, 13 (1985); G. U. Kulkarni, V. Vijayakrishnan, G. Ranga Rao, R. Seshadri, and C. N. R. Rao, Appl. Phys. Lett. 57, 1823 (1990).
[16]T. Tani, T. Itoh, and S. Tanaka, J. Phys. Soc. Jpn. 49, Suppl. A 309 (1980); S. Kondoh *et al.*, Solid State Commun. 67, 879 (1989).
[17]R. A. Schweinforth *et al.*, Appl. Phys. Lett. 61(4), 480 (1992).
[18]Z. Schlesinger and R. T. Collins, Mater. Res. Soc. Bull. 15, 44 (1990); J. M. Valles, Jr. and R. C. Dynes, *ibid.* 15, 51 (1990); R. C. Dynes *et al.*, Phys. Rev. Lett. 67, 509 (1991); F. Sharifi, A. Pargellis, R. C. Dynes, B. Miller, E. S. Helman, J. Rosamilia, and E. H. Hartford, Jr., Phys. Rev. B 44, 12 521 (1991); F. Sharifi, A. Pargellis, and R. C. Dynes, Phys. Rev. Lett. 67, 512 (1991).
[19]T. Hasegawa, H. Ikuta, and K. Kitazawa (unpublished).
[20]The negative-U, extended Hubbard model has also been studied earlier in the context of bipolaron mechanism for superconductivity (Ref. 42). For a recent review of earlier work on this model, especially in the large-U limit, see, e. g., R. Micnas, J. Ranninger, and S. Robaszkiewicz, Rev. Mod. Phys. 62, 113 (1990).
[21]S. Robaszkiewicz, R. Micnas, and K. Chao, Phys. Rev. B 26, 3915 (1982).
[22]A. Aharony and A. Auerbach, Phys. Rev. Lett. 70, 1874 (1993).
[23]K. S. Liu and M. E. Fisher, J. Low Temp. Phys. 10, 655 (1973).
[24]In an earlier calculation (Ref. 21) the superconducting order parameter was chosen to be a singlet only (b_s in our case). This choice is, however, not correct. We have shown here that, in the context of a negative-U, extended Hubbard model, both b_s and b_e are nonzero and the correct choice is Δ_s.
[25]I. Affleck *et al.*, Phys. Rev. B 38, 745 (1988).
[26]A. Taraphder and P. Coleman, Phys. Rev. Lett. 66, 2814 (1991).
[27]A. B. Migdal, Sov. Phys. JETP **1**, 996 (1958); R. Schrieffer, *Theory of Superconductivity* (Benjamin, New York, 1964), Chap. 7.
[28]P. W. Anderson, Phys. Rev. 86, 696 (1952).
[29]R. Schrieffer, X-G. Wen, and S. C. Zhang, Phys. Rev. Lett. 60, 944 (1988); Phys. Rev. B 39, 11663 (1989); T. Kostyrko, Phys. Status Solidi 143, 149 (1989).
[30]A. Zingh and Z. Tesanović, Phys. Rev. B 41, 614 (1990).
[31]A. L. Fetter and J. D. Walecka, *Qantum Theory of Many-Particle Systems* (McGraw-Hill, New York, 1971).
[32]A. I. Liechtenstein, I. I. Mazin, C. O. Rodriquez, O. Jepsen, O. K. Andersen, and M. Methfessel, Phys. Rev. B 44, 5388 (1991). The LDA ground-state calculation of Liechtenstein *et al.* is indifferent to whether the Bi *6s* orbital occupancies can be described in terms of a negative U or a positive U. The situation is somewhat similar to LDA calculations of La_2CuO_4 (Refs. 33 and 34), which give a qualitatively incorrect ground state. However, the existence of a large positive U in this system was inferred by Hybertsen, Schluter, and Christensen (Ref. 33) by doing an LDA calculation of energy as a function of *locally* constrained rf-electron number (Ref. 35). Similar calculations have not been carried out for $BaBiO_3$ and its derivatives. Therefore, the fact that an LDA calculation for $Ba_{1-x}K_xBiO_3$ leads to a small-gap semiconducting ground state with a structural distortion (at the correct value of x, but in a rigid-band approximation) but with no charge disproportionation, is not an argument against the existence of a local negative U. Further, the electronic-structure results are inconsistent with the observed electrical and optical gaps as we discuss in the text.
[33]M. S. Hybertsen, M. Schluter, and N. E. Christensen, Phys. Rev. B 39, 9028 (1989).
[34]A. K. McMahan, R. M. Martin, and S. Satpathy, Phys. Rev. B 38, 6650 (1989).
[35]An early calculation of negative U using LDA, but again with a local charge constraint and distortion coordinate as an extra degree of freedom, is that for Si vacancy, due to Baraff, Kane, and Schluter [G. A. Baraff, E. O. Kane, and M. Schluter, Phys. Rev. B 21, 5662 (1980)].
[36]C. J. Stanton and J. W. Wilkins, Phys. Rev. B 35, 9722 (1987).
[37]A. Taraphder and Sanjay Sarker (unpublished).
[38]H. Matsuda and T. Tsuneto, Prog. Theor. Phys. Suppl. 46, 411 (1970).
[39]D. N. Zubarev, Usp. Fiz. Nauk 71, 71 (1960) [Sov. Phys. Usp. 3, 320 (1960)].
[40]J. F. Federici, B. I. Greene, E. H. Hartford, and E. S. Hellman, Phys. Rev. B 42, 923 (1990).
[41]G. Ruani, A. J. Pal, C. Talianai, R. Zamboni, X. Wei, L. Chen, and Z. V. Vardeny, Synth. Met. 41-43, 3977 (1991).
[42]B. K. Chakraverty and J. Ranninger, Philos. Mag. 52, 669 (1985).